PB2000-102907

# *Evaluation of the Cause of Cracking in Bridge #MEG-124-6.78*

by
Richard A. Miller
Frank E. Weisgerber
Weiguo Zhang
Xuhua Dong
Andreas Greuel
Todd Long

Draft Final Report to the Sponsors:
Ohio Department of Transportation
Federal Highway Administration
October 1999

University of Cincinnati
Department of Civil and Environmental Engineering
P. O. Box 210071
Cincinnati, OH 45221-0071

The contents of this report reflect the views of the author, who is responsible for the facts and accuracy of the data presented herein. The contents do not necessarily reflect the official views or policies of the Federal Highway Administration or the Ohio Department of Transportation. This report does not constitute a standard, specification or regulation.

REPRODUCED BY: NTIS
U.S. Department of Commerce
National Technical Information Service
Springfield, Virginia 22161

PROTECTED UNDER INTERNATIONAL COPYRIGHT
ALL RIGHTS RESERVED.
NATIONAL TECHNICAL INFORMATION SERVICE
U.S. DEPARTMENT OF COMMERCE

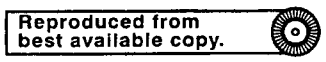

| 1. Report No. | 2. Government Accession No. | 3. Recipient's Catalog No. |
|---|---|---|
| FHWA/OH-99/014 | | |

| 4. Title and Subtitle | 5. Report Date |
|---|---|
| Evaluation of the Cause of Cracking in Bridge #MEG-124-6.78 | October, 1999 |
| | 6. Performing Organization Code |
| | 8. Performing Organization Report No. |
| 7. Author(s) | 10. Work Unit No. (TRAIS) |
| Richard A. Miller, Frank E. Weisgerber | |
| 9. Performing Organization Name and Address | 11. Contract or Grant No. |
| The University of Cincinnati<br>Department of Civil and Environmental Engineering<br>Cincinnati, OH 45221-0071 | State Job No. 14675(0) |
| | 13. Type of Report and Period Covered |
| | Final Report |
| 12. Sponsoring Agency Name and Address | 14. Sponsoring Agency Code |
| Ohio Department of Transportation<br>1600 West Broad Street<br>Columbus, OH 43223 | |

15. Supplementary Notes

Prepared in cooperation with the U.S. Department of Transportation, Federal Highway Administration

16. Abstract

Bridge MEG 124-6.78 was a single span, composite, adjacent, prestressed box girder bridge with a 45° right forward skew. After being in service about 1 year, the three edge beams on one side of the bridge showed extensive bottom flange cracking. Diagonal and vertical cracks were visible on the sides of the fascia beam. Beam specimens were removed from the bridge for destructive testing. The destructive testing showed that the diagonal cracks occurred as soon as the first flexural cracks began to appear. As load increased, the diagonal cracks grew larger, but the beams held over 445 kN (100 kips) total.

It was found that the cause of failure was construction error. These skewed boxes were detailed to have all the strand debonded from the end of the beam to the obtuse corner. The end of the beam has conventional reinforcing. This creates a straight (non-skewed) beam with a reinforced concrete triangle on the end. Unfortunately, the contractor debonded the strands past the obtuse corner to end of the mild steel, essentially creating an unreinforced section. This section failed under load, causing the diagonal cracks.

The bridge was rebuilt and tested. It was found to behave as a single unit and there was reasonable distribution of loads between the beams. The flexural stresses in the girder were very low. No diagonal cracking was observed. The testing confirmed that, properly constructed, the bridge was adequate.

Finally, finite element models of the bridge were constructed. The first model duplicated the "as built" condition of the original. This model confirmed the crack patterns shown in the actual test - diagonal cracking at the end of the girders. A second model was of the "as built" for the new bridge structure. The model confirmed that, properly constructed, the girders will not have diagonal cracking at the end. The last model was a combination of the first two. In this model, half the prestressing strands were debonded to the termination point of the mild steel. This model showed normal flexural cracking at the midspan, but also showed cracking at the ends.

| 17. Key Words | 18. Distribution Statement |
|---|---|
| Bridge, box girders, cracking, concrete, destructive testing, finite elements, load testing, prestressed | No Restrictions. This document is available to the public through the National Technical Information Service, Springfield, Virginia 22161 |

| 19. Security Classif. (of this report) | 20. Security Classif. (of this page) | 21. No. of Pages | 22. Price |
|---|---|---|---|
| Unclassified | Unclassified | | |

Form DOT F 1700.7 (8-72) Reproduction of completed page authorized

# Evaluation of the Cause of Cracking in Bridge #MEG-124-6.78

by
Richard A. Miller, Frank E. Weisgerber, Weiguo Zhang, Xuhua Dong, Andreas Greuel, Todd Long
University of Cincinnati, Department of Civil and Environmental Engineering
P. O. Box 210071
Cincinnati, OH 45221-0071

## EXECUTIVE SUMMARY

Bridge MEG 124-6.78 was a single span, composite, adjacent, prestressed box girder bridge with a 45° right forward skew. After being in service about 1 year, the three edge beams on one side of the bridge showed extensive bottom flange cracking. Diagonal and vertical cracks were visible on the sides of the fascia beam. Field tests done on the bridge in a previous study indicated that the cracking did not occur due to overload or improper load distribution.

Beam specimens were removed from the bridge for destructive testing. Two specimens were tested: one which had no cracking and one which was already cracked. The uncracked beam was tested first. Loading consisted of two point loads, one applied at 7 ft. from the support and one applied at 28 ft. from that same support. The destructive testing showed that the diagonal cracks occurred as soon as the first flexural cracks began to appear. As load increased, the diagonal cracks grew larger, but the beams held over 50 kips / load point (100 kips, total). The cracked beam was tested next and was found to have the same behavior as the uncracked beam.

It was found that the cause of failure was construction error. These skewed boxes were detailed to have all the strand debonded from the end of the beam to the obtuse corner. The end of the beam has conventional reinforcing. This creates a straight (non-skewed) beam with a reinforced concrete triangle on the end. Unfortunately, the contractor debonded the strands past the obtuse corner to end of the mild steel, essentially creating an unreinforced section. This section failed under load, causing the diagonal cracks.

The bridge was rebuilt and the new girders properly constructed. After the new bridge was constructed, it was tested. The bridge was found to behave as a single unit and there was reasonable distribution of loads between the beams. It was found that the flexural stresses in the girder were very low. No diagonal cracking was observed. The testing confirmed that, properly constructed, the bridge was adequate.

Finally, finite element models of the bridge were constructed. The first model duplicated the "as built" condition of the original bridge; the prestressing strands were debonded to the termination point of the mild steel. This model confirmed the crack patterns shown in the actual test - diagonal cracking at the end of the girders. A second model was of the "as built" for the new bridge structure. The model confirmed that, properly constructed, the girders will not have diagonal cracking at the end and that, under high loads, the beam will exhibit normal flexural cracking at the center of the girder. The last model was a combination of the first two. In this model, half the prestressing strands were debonded to the termination point of the mild steel. This model showed normal flexural cracking at the midspan, but also showed cracking at the ends.

## ABSTRACT

Bridge MEG 124-6.78 was a single span, composite, adjacent, prestressed box girder bridge with a 45° right forward skew. After being in service about 1 year, the three edge beams on one side of the bridge showed extensive bottom flange cracking. Diagonal and vertical cracks were visible on the sides of the fascia beam. Field tests done on the bridge in a previous study indicated that the cracking did not occur due to overload or improper load distribution.

Beam specimens were removed from the bridge for destructive testing. Two specimens were tested: one which had no cracking and one which was already cracked. The uncracked beam was tested first. Loading consisted of two point loads, one applied at 7 ft. from the support and one applied at 28 ft. from that same support. The destructive testing showed that the diagonal cracks occurred as soon as the first flexural cracks began to appear. As load increased, the diagonal cracks grew larger, but the beams held over 50 kips / load point (100 kips, total). The cracked beam was tested next and was found to have the same behavior as the uncracked beam.

It was found that the cause of failure was construction error. These skewed boxes were detailed to have all the strand debonded from the end of the beam to the obtuse corner. The end of the beam has conventional reinforcing. This creates a straight (non-skewed) beam with a reinforced concrete triangle on the end. Unfortunately, the contractor debonded the strands past the obtuse corner to end of the mild steel, essentially creating an unreinforced section. This section failed under load, causing the diagonal cracks.

The bridge was rebuilt and the new girders properly constructed. After the new bridge was constructed, it was tested. The bridge was found to behave as a single unit and there was reasonable distribution of loads between the beams. It was found that the flexural stresses in the girder were very low. No diagonal cracking was observed. The testing confirmed that, properly constructed, the bridge was adequate.

Finally, finite element models of the bridge were constructed. The first model duplicated the "as built" condition of the original bridge; the prestressing strands were debonded to the termination point of the mild steel. This model confirmed the crack patterns shown in the actual test - diagonal cracking at the end of the girders. A second model was of the "as built" for the new bridge structure. The model confirmed that, properly constructed, the girders will not have diagonal cracking at the end and that, under high loads, the beam will exhibit normal flexural cracking at the center of the girder. The last model was a combination of the first two. In this model, half the prestressing strands were debonded to the termination point of the mild steel. This model showed normal flexural cracking at the midspan, but also showed cracking at the ends.

## ACKNOWLEDGEMENTS

This work was funded by the Ohio Department of Transportation and the Federal Highway Administration. The author would like to thank Mr. Roger Green, Mr. Vik Dalal and Mr. Lloyd Welker, all of the ODOT Central Office. Thanks are also due to Mr. Larry Coler and Mr. Doug Briggs, both of ODOT District 10. District 10 was also kind enough to provide the dump trucks for loading the bridge.

## TABLE OF CONTENTS

THIS PAGE INTENTIONALLY LEFT BLANK

# CHAPTER 1

# DESCRIPTION OF THE BRIDGE AND TESTING PROGRAM

## 1.1 Description of the Bridge

Bridge MEG - 124 - 6.78 is located in Meigs County, Ohio on State Route 124, just east of the town of Salem Center. Built in 1994, this structure is a single span, composite, adjacent box girder bridge consisting of nine box girders (eight CB21-48 and one CB21-36) with a 5.5" thick composite deck (Figures 1.1 and 1.2). The bridge has a 45'-0" span and a 45° right forward skew. Because it is on a curve, the bridge has a standard superelevation.

The bridge runs northwest to southeast (Figure 1.2), thus having a NW bound lane and a SE bound lane. For convenience, the beams have been numbered. Beam #1 is on the NE edge of the bridge under the NW bound lane. Beam #9 is on the SW edge under the SE bound lane (Figure 1.1).

In May, 1995, Malloon's Run (the creek under the bridge) flooded, covering the bridge with water. After the flood, a neighboring property owner checked the bridge and noticed cracking near the support (note: this is not to imply that the flooding caused the cracking; only that the flooding was the impetus which caused the neighbor to inspect the bridge). He notified ODOT District 10. District 10 engineers immediately inspected the bridge and found diagonal cracking at the obtuse corner of beam #9 (Figure 1.3). Additional, less severe, cracking was found near the acute corner of the beam. In all, the inspection revealed the following problems:

1) The beam on the southwest edge (numbered 9 in Figure 1.1 and shown in Figure 1.3) had diagonal cracks and straight cracks in the exposed side of the beam. These cracks continued to the bottom of the box where they became transverse (perpendicular to the span). Whether the cracks continued up the other side of the beam was not clear as the other side of the beam (being up against the the adjacent beam) was not visible. The worst cracking occurred at the northwest corner where the cracks appeared to be diagonal shear cracks. Less severe cracking, which appeared to a vertical flexural crack, occurred at the other end of the beam as well. In both cases, the cracks formed about 4 ft. from the obtuse corner.

2) Each of the adjacent beams (numbered 7 and 8 in Figure 1.1) had transverse cracks along the bottom. The sides of the beam were not visible so it could not be ascertained if the diagonal cracks existed along the sides of the beam. Again, cracking occurred at both ends of the beams approximately 4 ft. from the obtuse corner.

3) The abutments were poorly finished. Due to the superelevation of the structure, the top of the abutments should have had a constant slope. However, the slope was not constant causing the abutment to have a "wavy" appearance.

4) The bearing pads were not tight. It was possible to pull bearing pads out from under some of the beams.

5) The approach slab in the SE corner of the bridge (in the NW bound lane) had a large bump.

Due to the observed problems with the bridge, the engineers elected to close the SE bound lane (which passed over the cracked beams) while the cause of cracking was investigated and until the bridge could be replaced.

ODOT Engineers decided the first course of action would be to test the bridge under static and dynamic traffic loads and then, during replacement, remove beam specimens for later destructive testing. To this end, investigators from the University of Cincinnati were called upon to conduct the testing.

## 1.2 Testing and Analysis Program

In order to determine the cause of cracking in the beams, a three part testing program was designed. The three phases were:

1) Testing the existing structure as a unit under both static and dynamic truck loads.

2) It was clear that due to the severe cracking, the superstructure beams would need to be replaced. Some of the beams were salvaged and taken to Cincinnati for destructive load testing.

3) After replacement, the new superstructure was subjected to static truck loading, similar to that done in part 1.

Part 1 is described was completed under a previous project and is found in the report *Instrumentation of Bridge #MEG-124-6.78*. Parts two and three are described in this report.

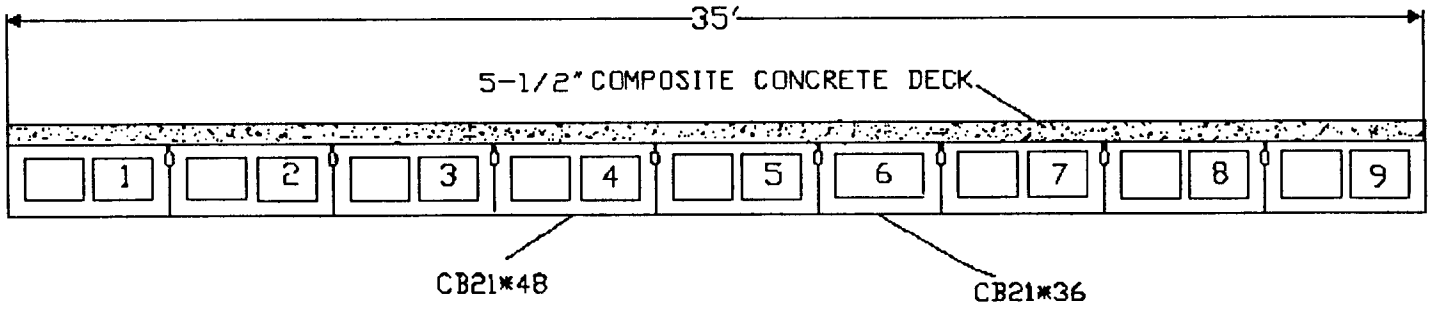


**Figure 1.1 - Bridge Cross Section**

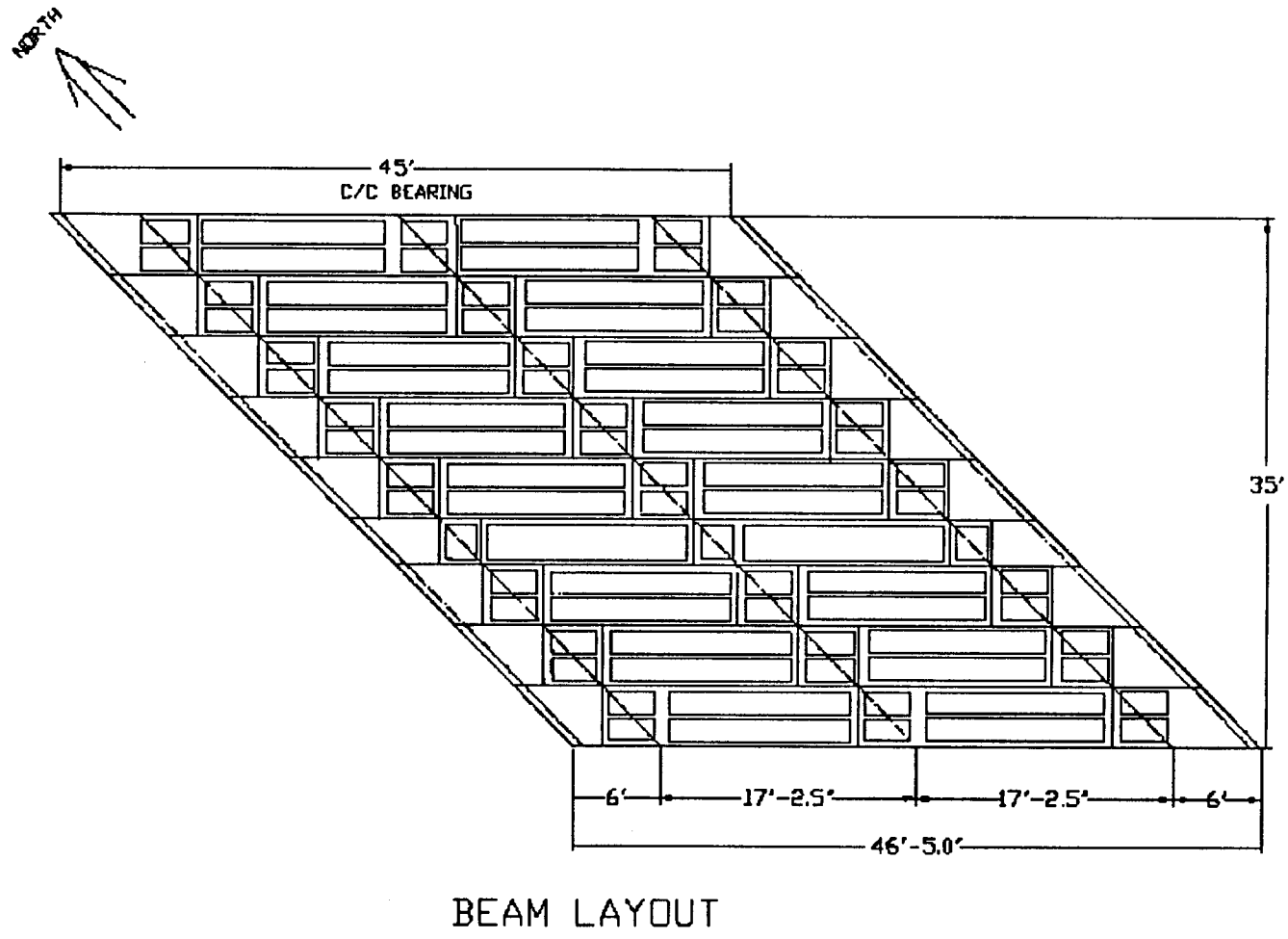


**Figure 1.2 - Bridge Plan**

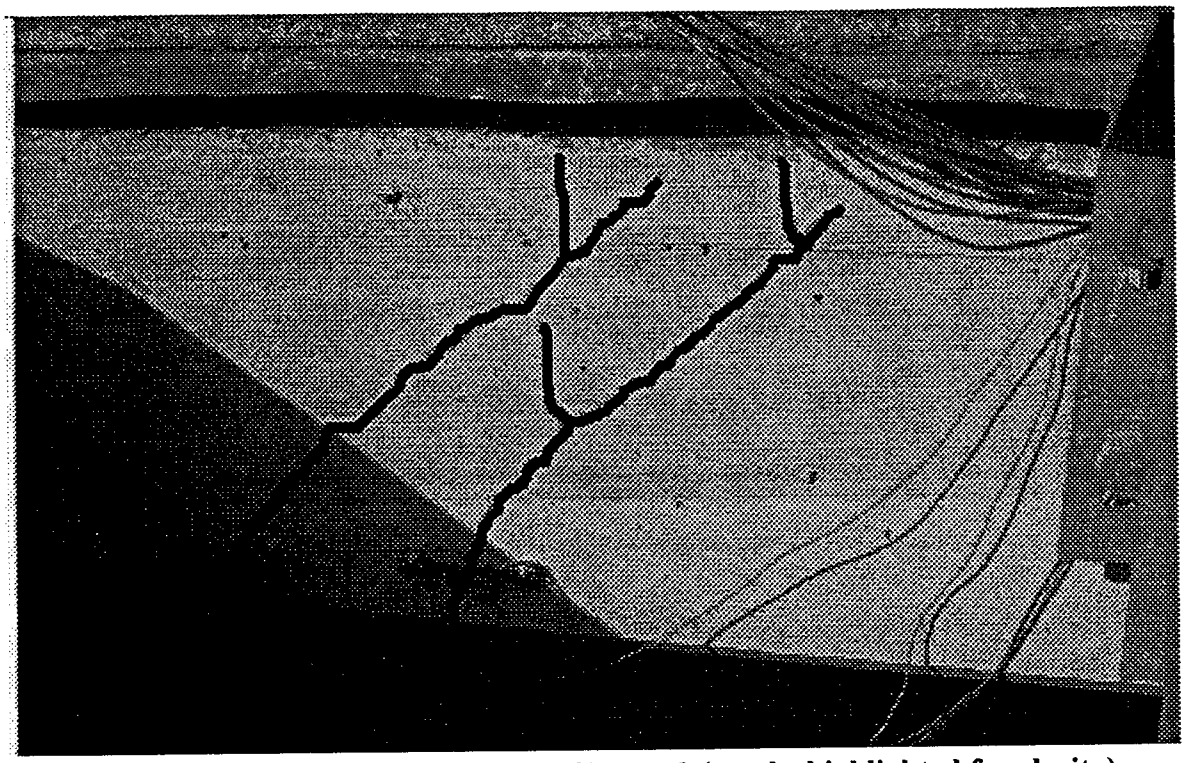

**Figure 1.3 a - Cracks at Northwest End of Beam 9 (cracks highlighted for clarity)**

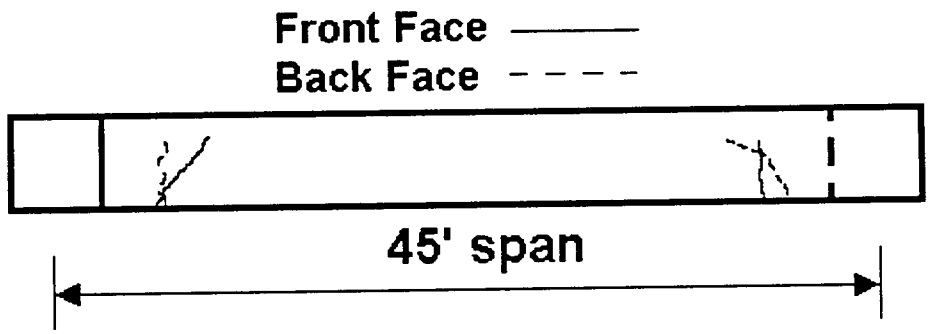


**Typical Crack Pattern - Beam 7, 8, 9**

**Figure 1.3 b - Crack Patterns**

THIS PAGE INTENTIONALLY LEFT BLANK

# CHAPTER 2

# CONCLUSIONS FROM PREVIOUS TESTING

## 2.1 Summary of Previous Testing

In an attempt to determine the cause of cracking, the original, cracked bridge was subjected to both static and dynamic truck load testing. For this testing, up to four dump trucks were used to apply load. Each truck had two single axles and a total weight of approximately 30 kips. The static and dynamic tests are summarized in the report *Instrumentation of Bridge #MEG-124-6.78*. While this testing could not determine the cause of failure, it did eliminate several possibilities.

## 2.2 Conclusions of the Previous Work

Based on the test results:

1) Under 10 different static load combinations, the bridge showed the expected the load distributions between the beams. Uniform loads were equally shared while loads which were more toward one edge were distributed more to that edge of the bridge, but the distribution was still reasonable. It did not appear that one or two beams were carrying the entire load. Therefore, the cause of failure was not overload in the edge beams due to improper load distribution.

2) Due to construction errors, the top of the abutments were not even and the bearing pads were not shimmed. Some of the bearing pads were loose and easily removed. Under load, the end of the beam with the loose pads twisted. Also, some twist was noted at the obtuse corners of the bridge due to the skew. However, the amount of twist was not enough to generate significant torsional shear stresses. Finite element analysis showed the total St. Vennant and warping shear stresses were about 75 psi. Therefore, torsion due to loose bearing pads did not cause the failure.

3) Dynamic testing was done by running a full dump truck over the bridge at 15, 30 and 45 mph. The dynamic magnification factor (impact) was measured as the maximum dynamic midspan deflection in the beams divided by the maximum static deflection for the same beam. The maximum dynamic magnification factor was 30%. This is consistent with the value used in the AASHTO *Standard Specifications*.

4) The bridge was on a coal route. The effect of coal trucks running over the bridge was assessed. It was found that coal trucks had the effect of being about twice as heavy as the dump trucks. This is consistent with previous ODOT weigh-in-motion measurements and would also be consistent with the alternate military design loading. The coal trucks had a dynamic magnification factor of about 35%. The design impact factor is taken as 30% maximum, but this higher impact factor is within the range of experimental accuracy.

Therefore, it does not appear the bridge failed due to heavy coal trucks.

5) The original bridge design used the *AASHTO Standard Specifications for Highway Bridges*. These specifications do not have separate distribution factors for shear or account for skew in the member. A 1994 *AASHTO Guide Specification* has separate distribution factors for shear and accounts for skew. When the bridge is analyzed under the *Guide Specification*, the wheel load shear distribution factor rises from 0.698 to 1.05. However, if the beams are analyzed using the higher distribution factor, a 30% impact and allowing for 20% overload, the beams are still safe in shear.

The results of these tests show that beam failure did not occur due to normal traffic overloading the bridge. To find the cause of failure, additional work is needed.

# CHAPTER 3

# REMOVAL OF THE SPECIMENS AND DESTRUCTIVE TESTING

## 3.1 Removal of the Specimens

After the truck load testing from Phase I was complete, the bridge structure was replaced with a new, duplicate structure (See Chapter 4 for details on the replacement structure). When the existing bridge was removed, 4 specimens were taken - two cracked and two intact. Unfortunately, the contractor attempted to remove the #9 beam without guidance from ODOT or UC and damaged it. (See Figure 1.1 for numbering). Therefore, the cracked beams taken for testing were #7and #8. The two intact beams taken for testing were #3 and #5. This provided two test specimens and two spare specimens.

The beam removal process was determined by the contractor in consultation with the UC Research Team, ODOT District 10 and the ODOT Department of Structural Engineering. This process was:

1) The contractor carefully measured the position of the joints between the beams from underneath and transferred these measurements to the top, composite slab. Using a concrete saw, the contractor carefully cut through the composite slab, the shear keys and the tie rods.

2) Because the beams were adjacent, it was not possible to put lifting straps around the beams to lift them. Holes were drilled in each end of the beam near the abutments and 1" diameter threaded rods were embedded approximately 6" into the holes and epoxied in place. Lifting lugs were attached to rods and two cranes lifted the beams just enough to slide them slightly sideways, creating a gap between the beams so that lifting straps could be placed around the beams (Figure 3.1).

3) For the cracked beams, steel angle "bandages" were placed over the crack to prevent damage during the lifting process (Figure 3.2).

4) The beams were lifted onto flat bed trucks and transported to Cincinnati.

On removal, the hidden sides of the #7, #8 and #9 beams could be inspected. It was found that all three beams had the same crack pattern. Diagonal cracks occurred approximately 4 ft. from the obtuse corners and on the exact opposite face of the beams there were vertical flexural cracks, some of which had started to turn into diagonal cracks. (Figure 3.3).

## 3.2 Destructive Testing

The beams were taken to the Prestress Services, Inc. plant in Melbourne, Kentucky (this is approximately 16 mi. south of Cincinnati). The University of Cincinnati, Department of Civil and Environmental Engineering maintains a testing facility on this site. This facility consists of two, 100 kip capacity testing frames placed 21 ft. apart. The position of the frames is fixed. Along with the testing frames, the test facility also has the required hydraulic pumps, cylinders, control valves and computerized data acquisition systems required for beam testing (Figure 3.4).

Since the cracks at the end of the beam appeared to be shear induced, the beams were loaded to induce maximum shear at the point of the crack. Cracking occurred between 4 - 6 ft. from the obtuse corner, so one load point was placed 5 ft. from one randomly chosen obtuse corner. The other load point then fell 26 ft. from that same obtuse corner and was 15 ft. from the other obtuse corner (Note: The beam span was 45 ft. and with a 45 ° skew, thus the obtuse corners were 41 ft. apart. See Figure 3.5 for load placement).

This load position was chosen for another reason. When a simple span is loaded under point loads, the moment is maximum when the loads are placed such that the midspan of the beam is exactly halfway between the centroid of the loads and the nearest point load. For two point loads on this 45 ft. span, the moment is maximized by placing the loads at 5 ft. and 26 ft. from one obtuse corner. Thus, this load placement caused maximum shear at one end and maximum midspan moment.

**Important Note:** For the purpose of determining where loads were applied and where cracks occurred, compass directions will be used. The beam was placed such that its long axis ran east/west. The load applied near the support was applied near the west support (Figure 3.5) .

## 3.3 Testing of an Uncracked Beam

An uncracked beam (Beam #5, Figure 1.1) was tested first. The beam was loaded in displacement control with the cylinder closest to midspan applying load such that the beam was deflected in increments of 0.05 in. at the load point. In the elastic range, this applied load in increments of approximately 2 kips at each load point.

At a load of 23 kips at each load point, a flexural crack formed at midspan and flexural cracks also formed at the east end (the end away from the load) on both sides of the beam. On the next increment of load (approximately 25 kips per load point), flexural cracks formed at the west end; again on both sides of the beam. Subsequent load increments caused these flexural cracks at the ends to become diagonal (Figure 3.6). The cracks on both sides were connected by a crack through the bottom flange. Some additional midspan cracking was noted, but it was minimal.

The test was continued until a load of 52 kips had been applied at each load point. By this time, the cracks at each end had begun to open wide and there was significant spalling of the concrete from the crack in the bottom flange. The test was stopped for safety reasons.

After the test, the spalled concrete was knocked off the bottom of the beam and a startling discovery was made. The cracking occurred exactly at the point where the mild steel was terminated, however, it was also found that all of the strands, except for one, had been debonded to the same termination point (Figure 3.7). By breaking off concrete at the end of the beam, it was determined that the strands had been debonded from the end of the beam to the termination point of the mild steel. The cause of failure was clearly that the section was unreinforced at this point. The only bonded strand was the one closest to the obtuse corner.

Figures 3.8 shows the instrumentation plan of the beam. This figure shows that deflection measurements were taken at the midspan of the beam and at each load point. Figures 3.9 -11 show the load- deflection graphs for east load point of the beam, midspan and west load point, respectively. For comparison, corresponding load deflection graphs created by the *RESPONSE* program are also shown. These computer generated graphs assume normal flexural failure. It appears that the real beam is stiffer than predicted at the east load point and the midspan (recall that these points are very close to each other), however this apparent extra stiffness is caused by shear cracking - the beam is not bending in a circular arc, but rather the center is displacing almost as a rigid body. This can be seen by the excessive deflection at the west load point (Figure 3.11) and from the deflection profiles in Figure 3.12.

In looking at Figures 3.9-11, it is amazing that this beam held as much load and was as ductile as it was, in spite of having a section which was, for all intents and purposes, an unreinforced section.

## 3.4 Testing of a Cracked Beam

Beam #7 (Figure 1.1), which was already cracked, was tested after the uncracked beam. The testing setup, testing procedure, load placement and instrumentation was exactly the same as in the uncracked beam test.

In this test, propagation of the existing cracks did not begin until a load of about was applied at each point. The first flexural cracking was found at 23 k/load point. The behavior of the two beams was consistent as can be seen by the load - deflection diagrams shown in Figures 3.13-15.

## 3.4 Cause of Failure

The results of destructive testing showed that the cause of failure was a fabrication error. It appears that the fabricator accidently debonded all but one strand to the end of the mild steel (Figure 3.16), creating an unreinforced section at this point.

In the original structure, the #7, #8 and #9 beams cracked. These beams were on the southwest side of the structure (Figure 3.17), on the inside of the curve. The lane over these beams carried the full coal trucks traveling toward Rutland. It is probable that these full coal trucks tried to "cheat" the curve by traveling down in the shoulder area of the beam (this would allow higher speeds by reducing the radius of their turn). When the trucks drove down in the shoulder area, the

entire load was concentrated on the three outside beams. Normally, the beams would have handled the load without problems, but since there was an unreinforced section, this section cracked under the large loads applied by the coal truck.

This scenario also explains why the beams on the northeast side of the bridge did not crack. Trucks traveling on this side of the bridge (toward Salem Center) were empty so they applied much less load. Also, trucks using the northwest bound lane would naturally "cheat" the curve by driving closer to the centerline, thus allowing more beams to share the load.

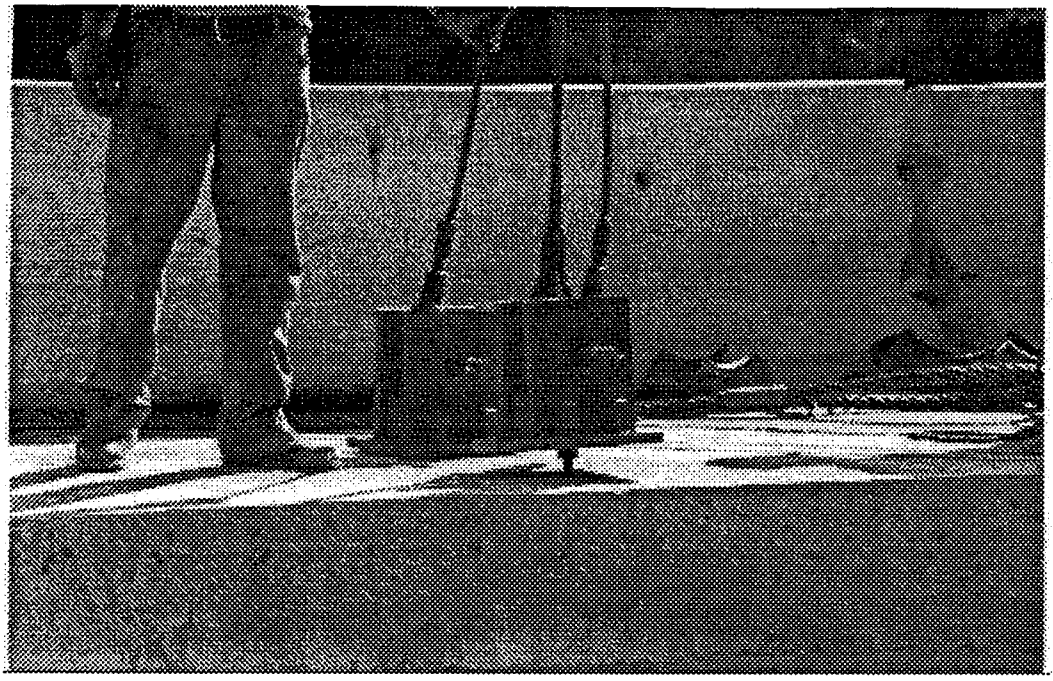

**Figure 3.1 - Moving the beams after cutting the joints.**

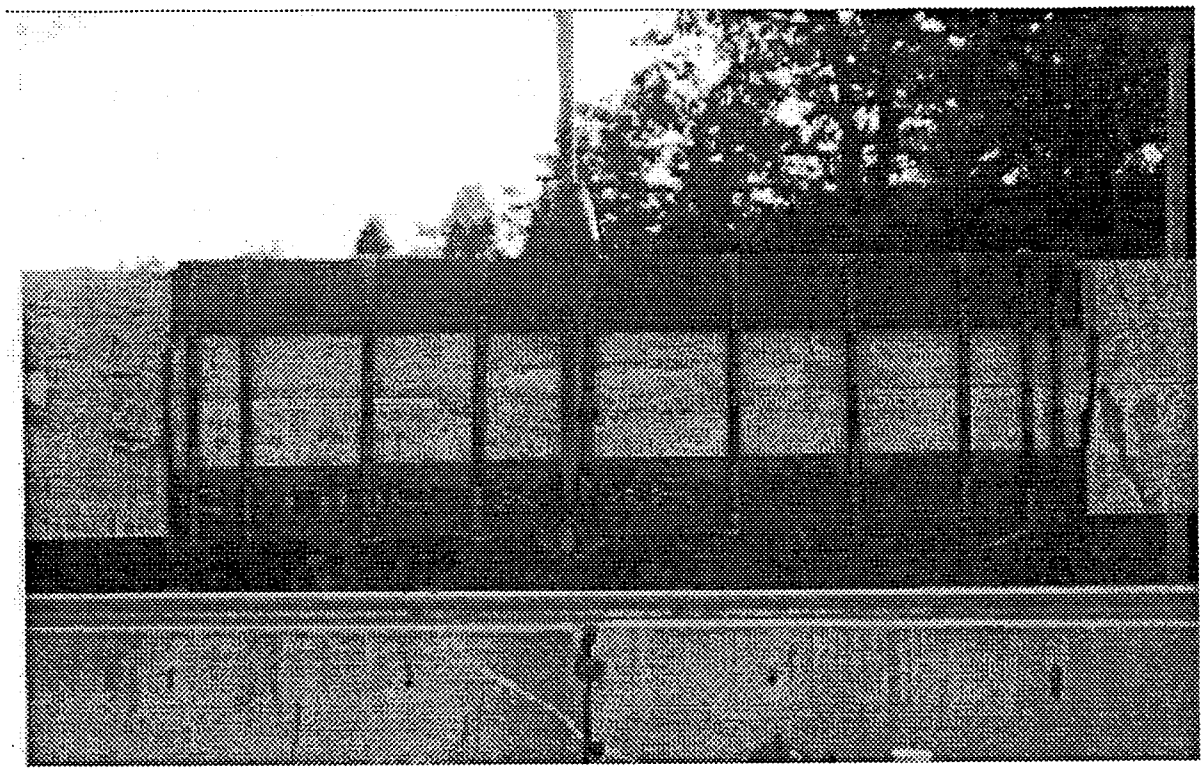

**Figure 3.2 - Bandage to protect the cracks during lifting and transport.**

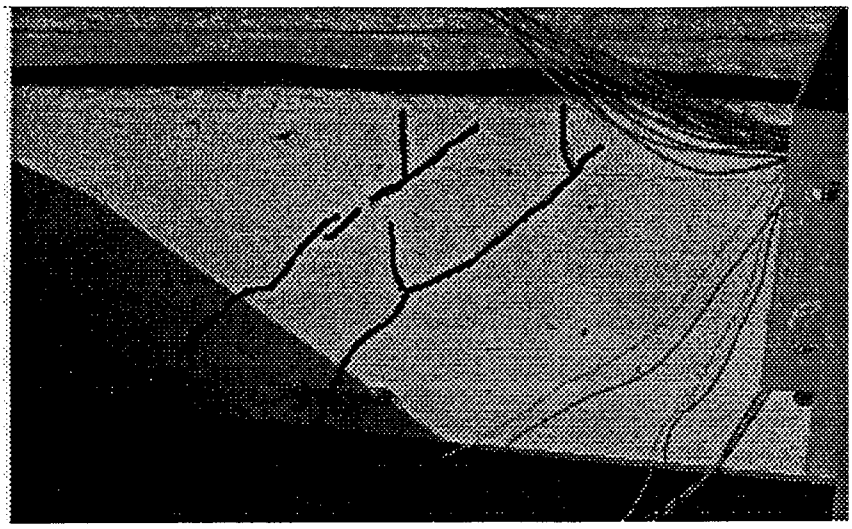

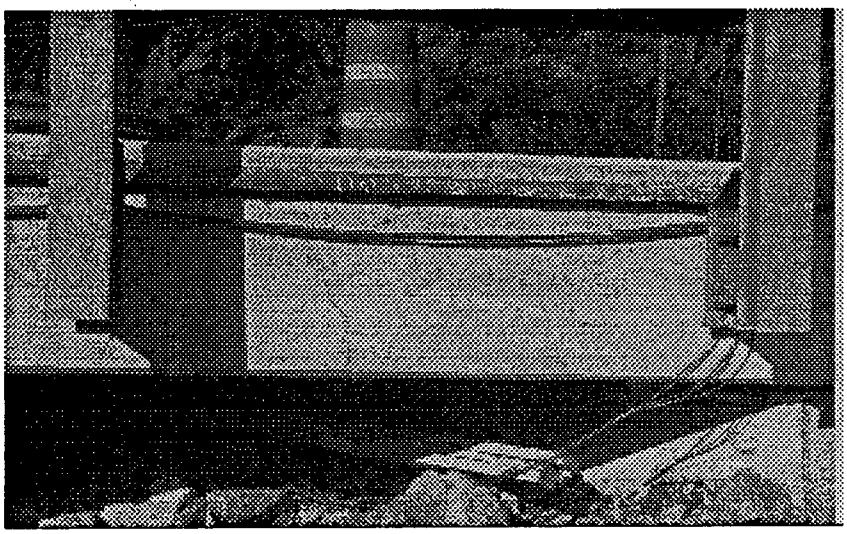

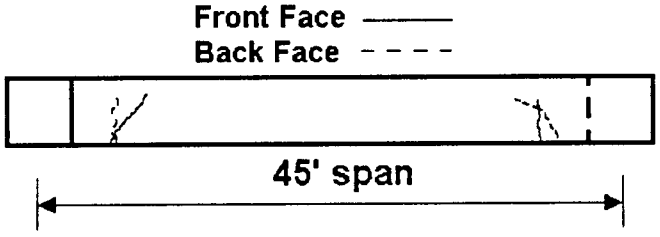


**Typical Crack Pattern - Beam 7, 8, 9**

**Figure 3.3 - Cracks in beams. Top - Cracks at NW end of beam #9, Middle - Cracks at SE end of beam #9, Bottom - Typical crack patterns in beams 7, 8, 9.**

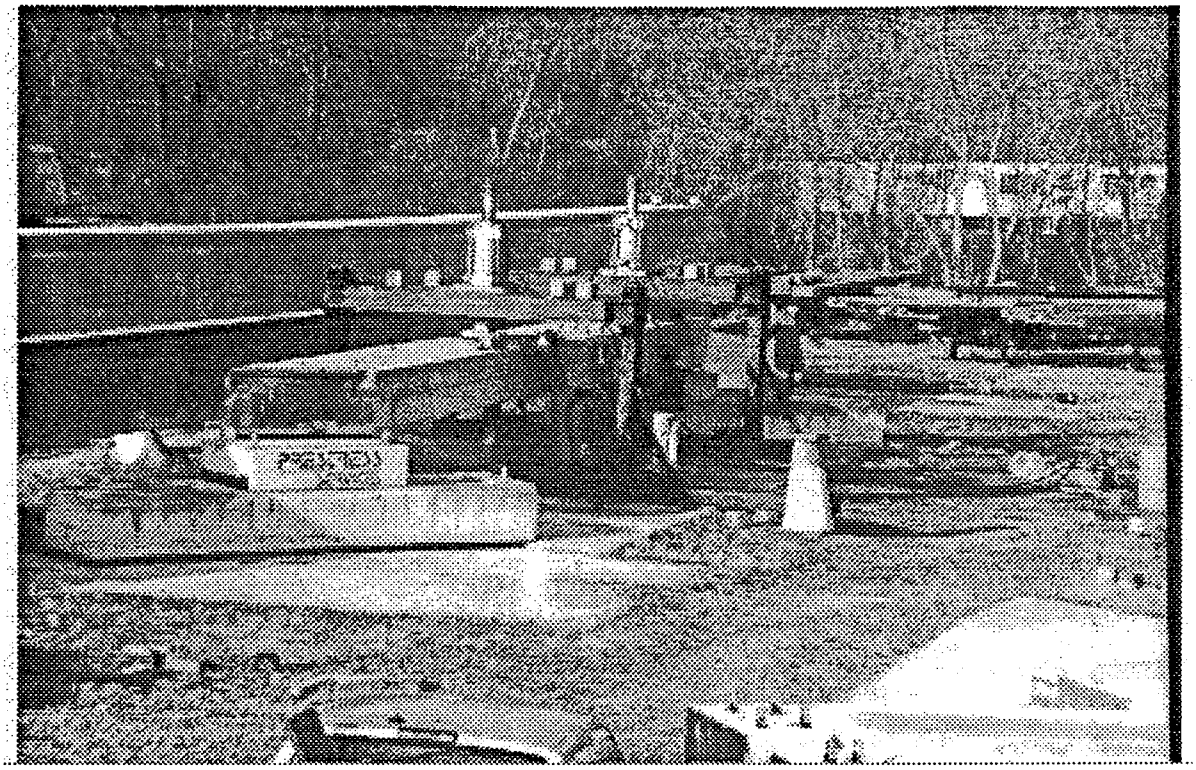

**Figure 3.4 - Testing frame**

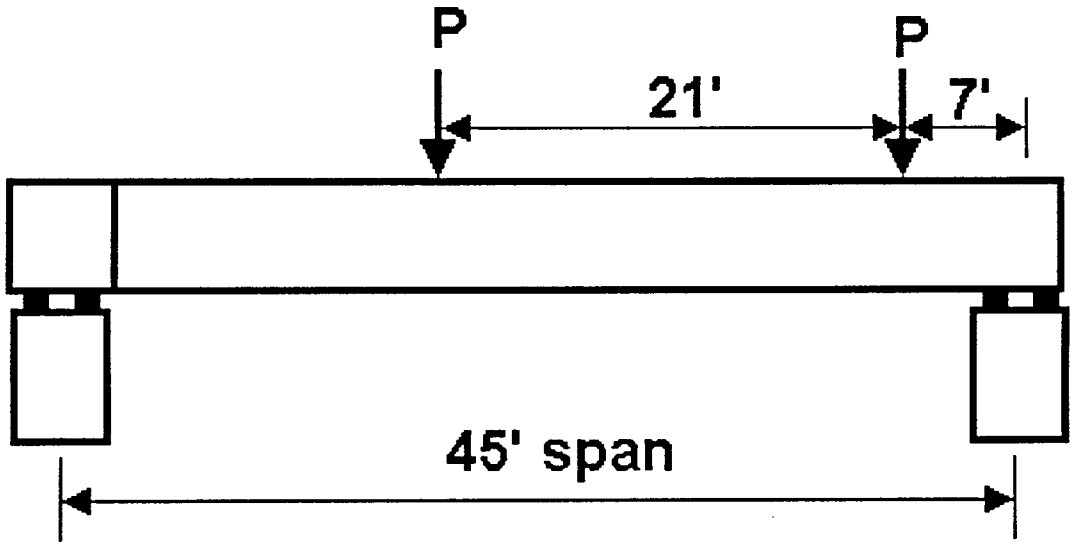


**Figure 3.5 - Load placement**

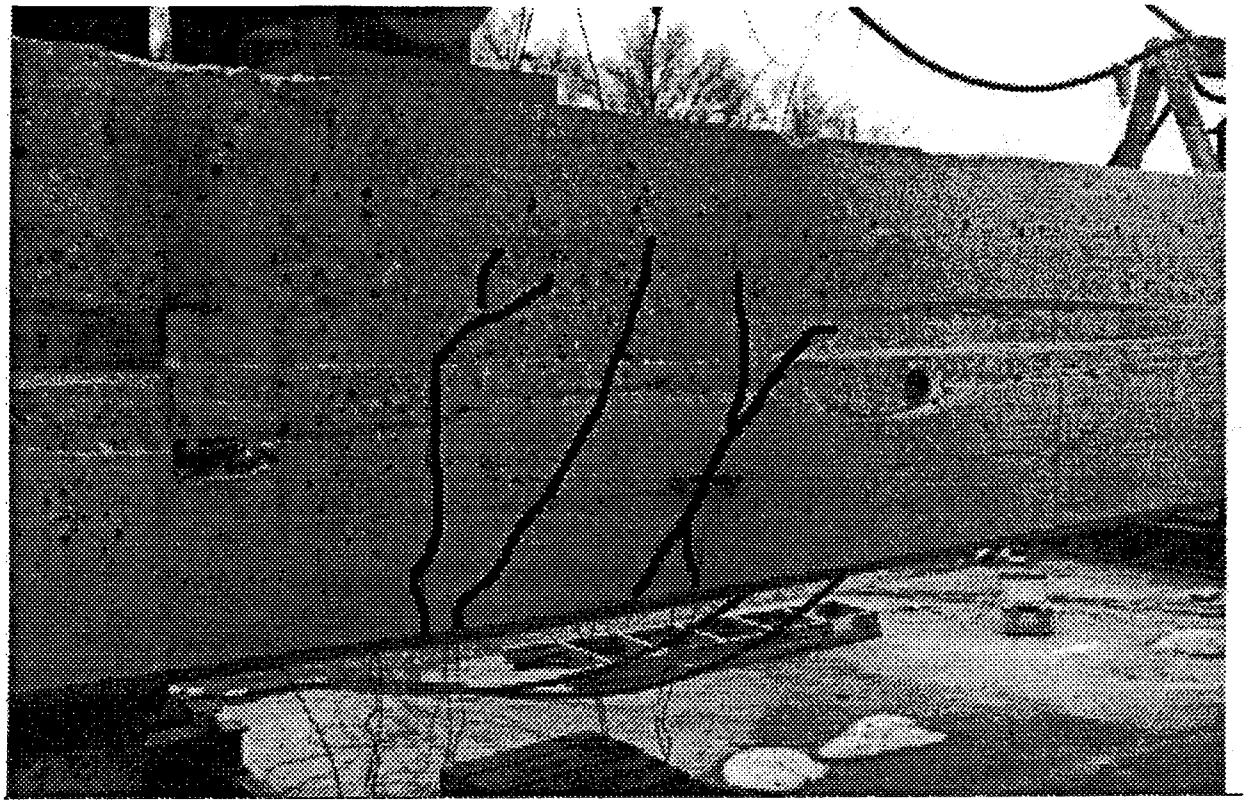

**Figure 3.6 - Typical diagonal crack formation (cracks enhanced)**

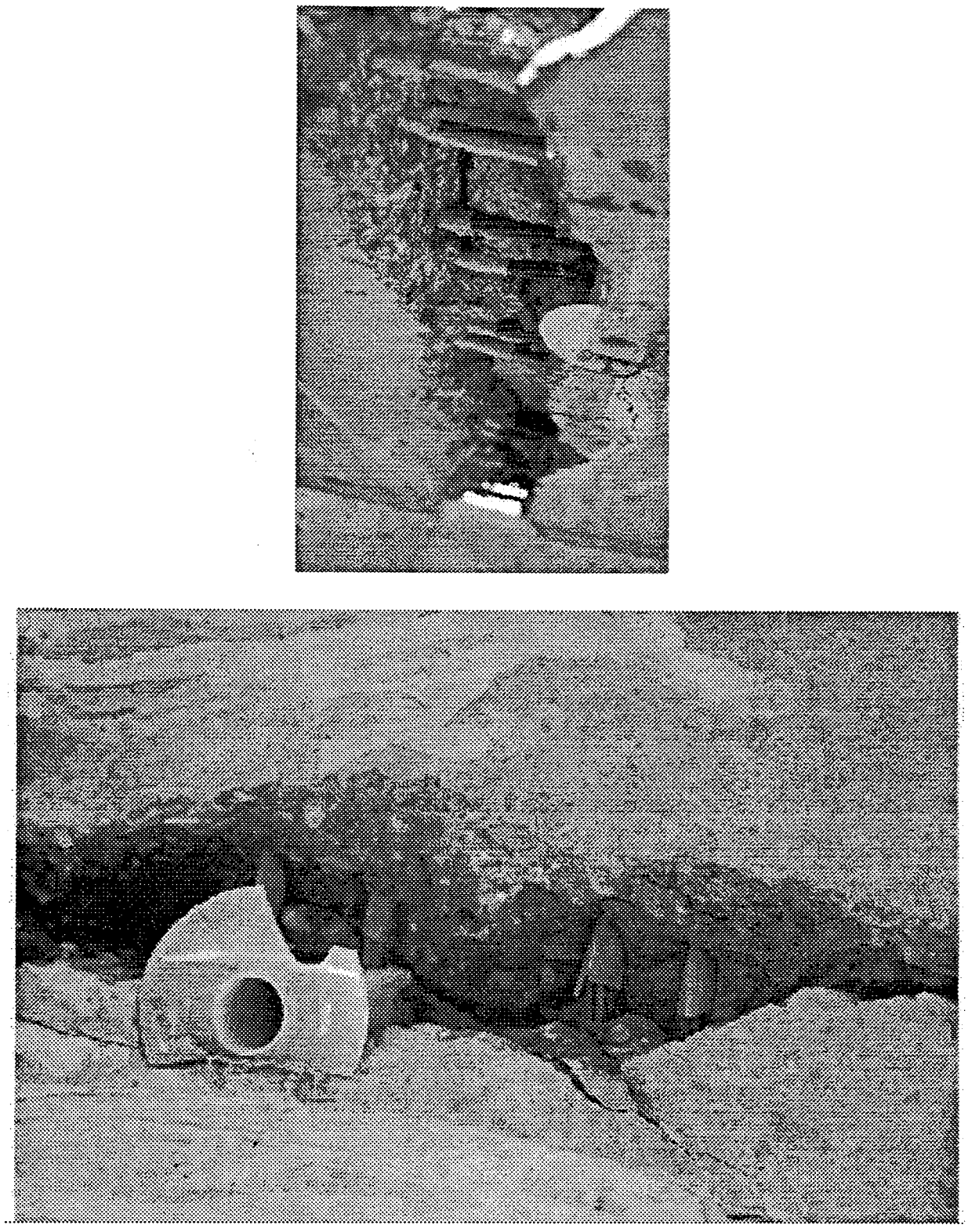

**Figure 3.7 - Failure surface. Note end of debonding sleeves.**

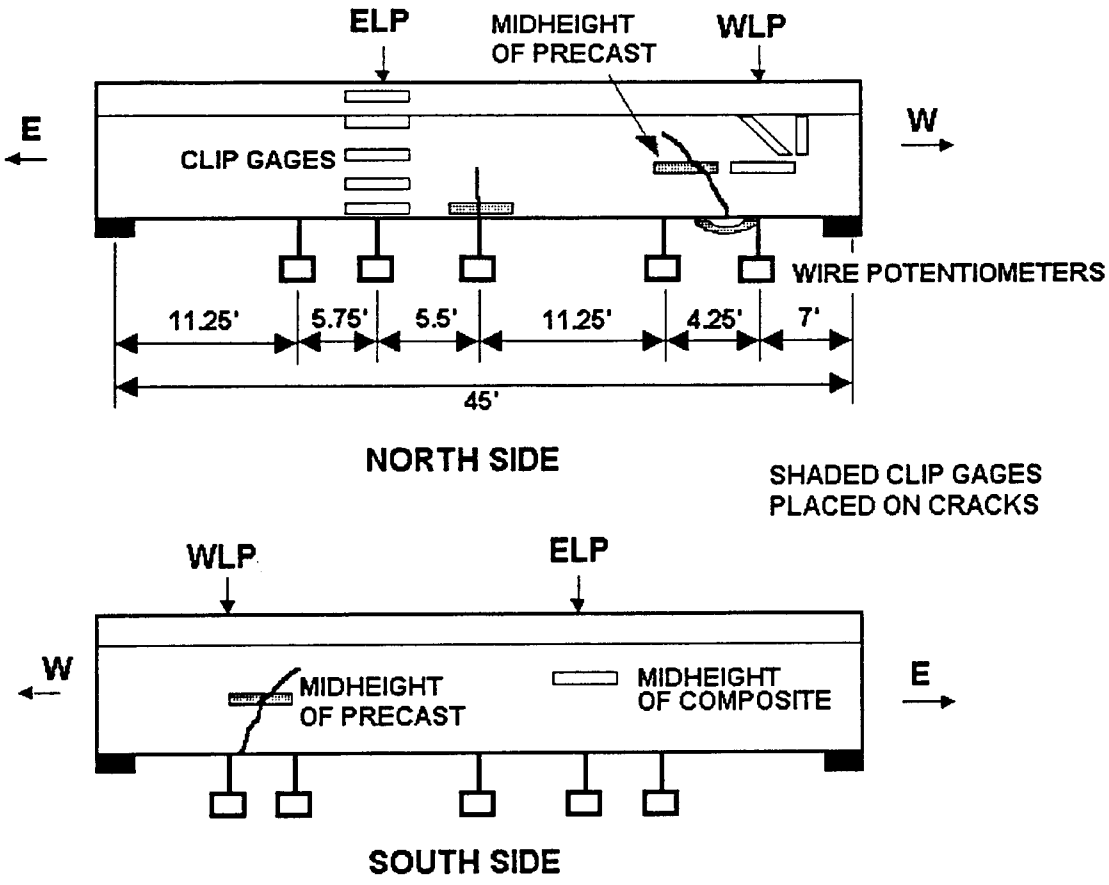


**Figure 3.8 - Instrumentation plan for destructive test.**

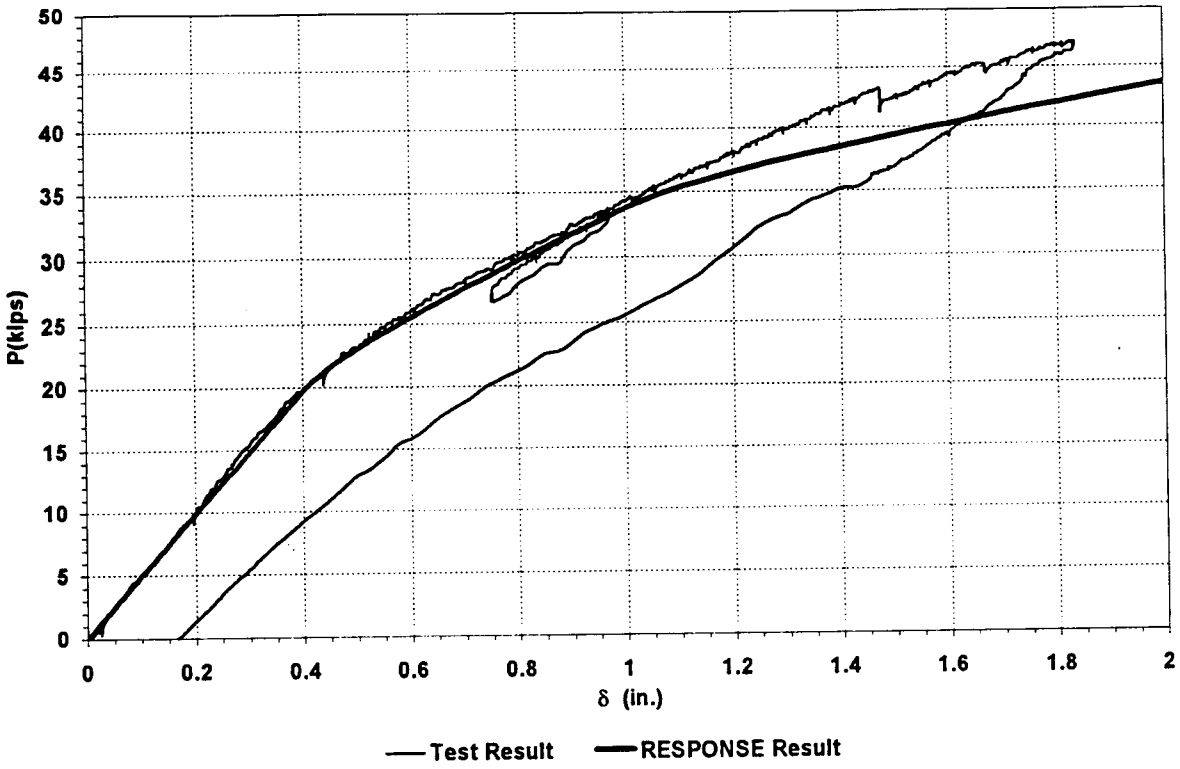


**Figure 3.9 - Load vs. deflection - east load point - uncracked beam**

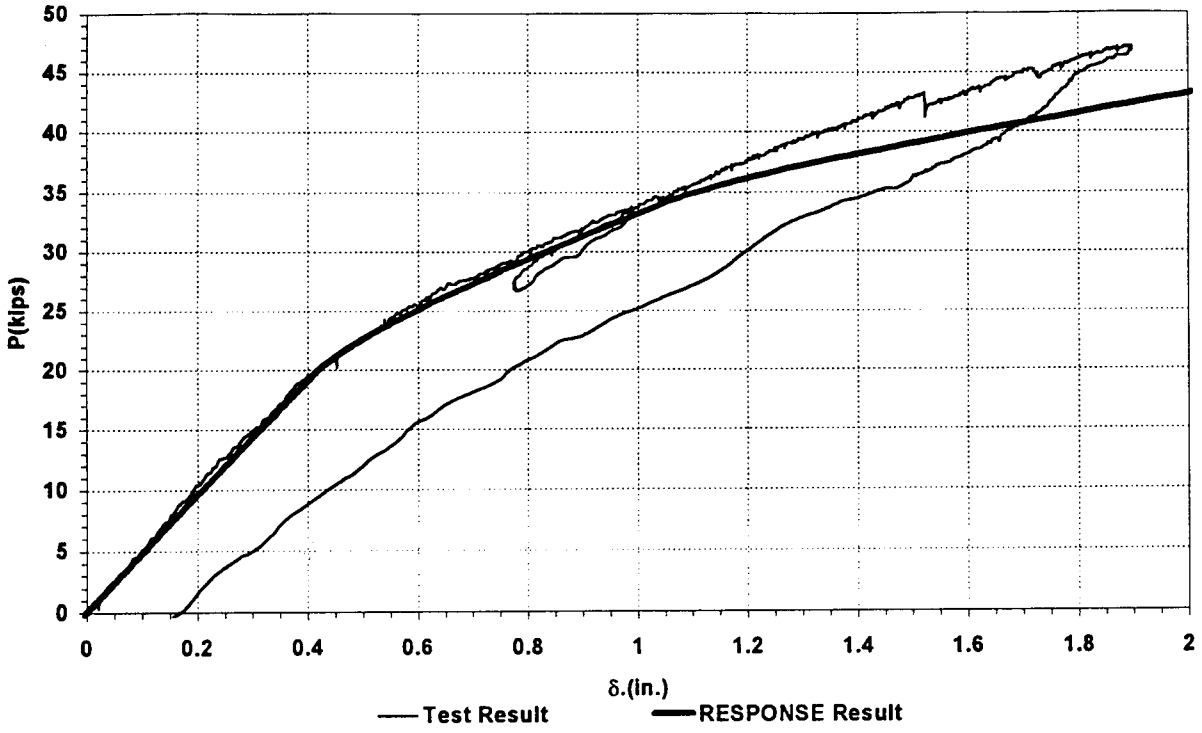


**Figure 3.10 - Load vs. deflection - midspan - uncracked beam.**

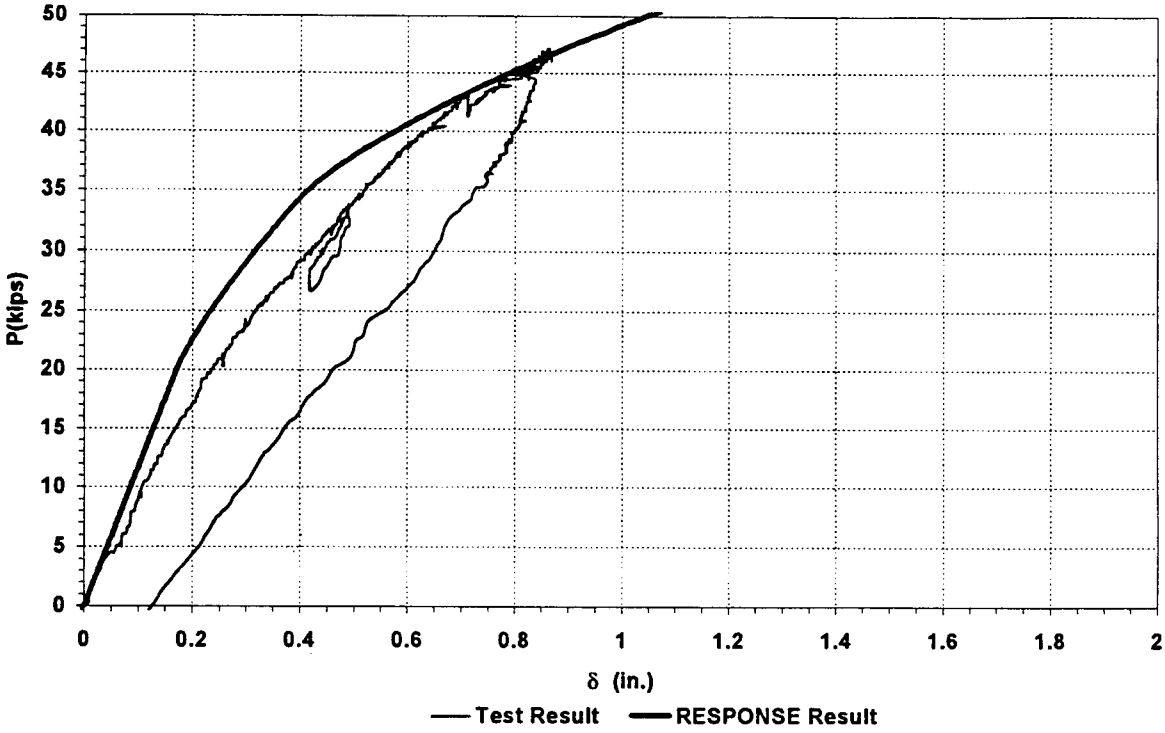


**Figure 3.11 - Load vs. deflection - west load point - uncracked beam.**

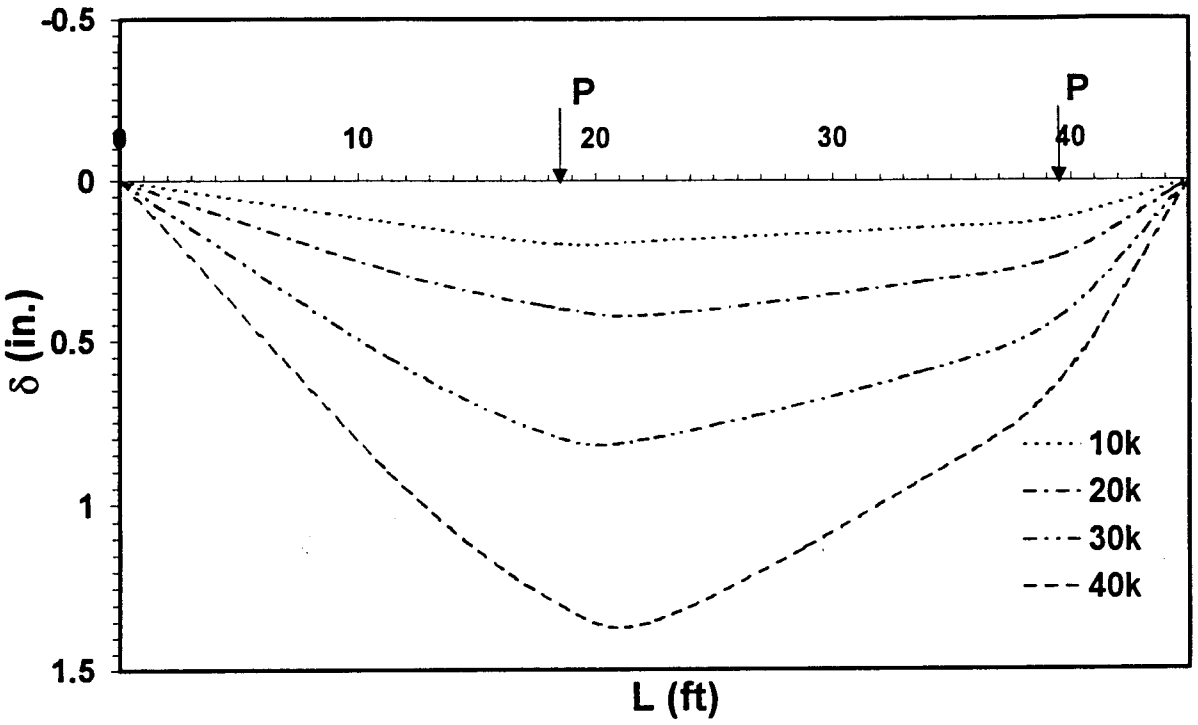


**Figure 3.12 - Deflection profiles of the uncracked beam - loads shown.**

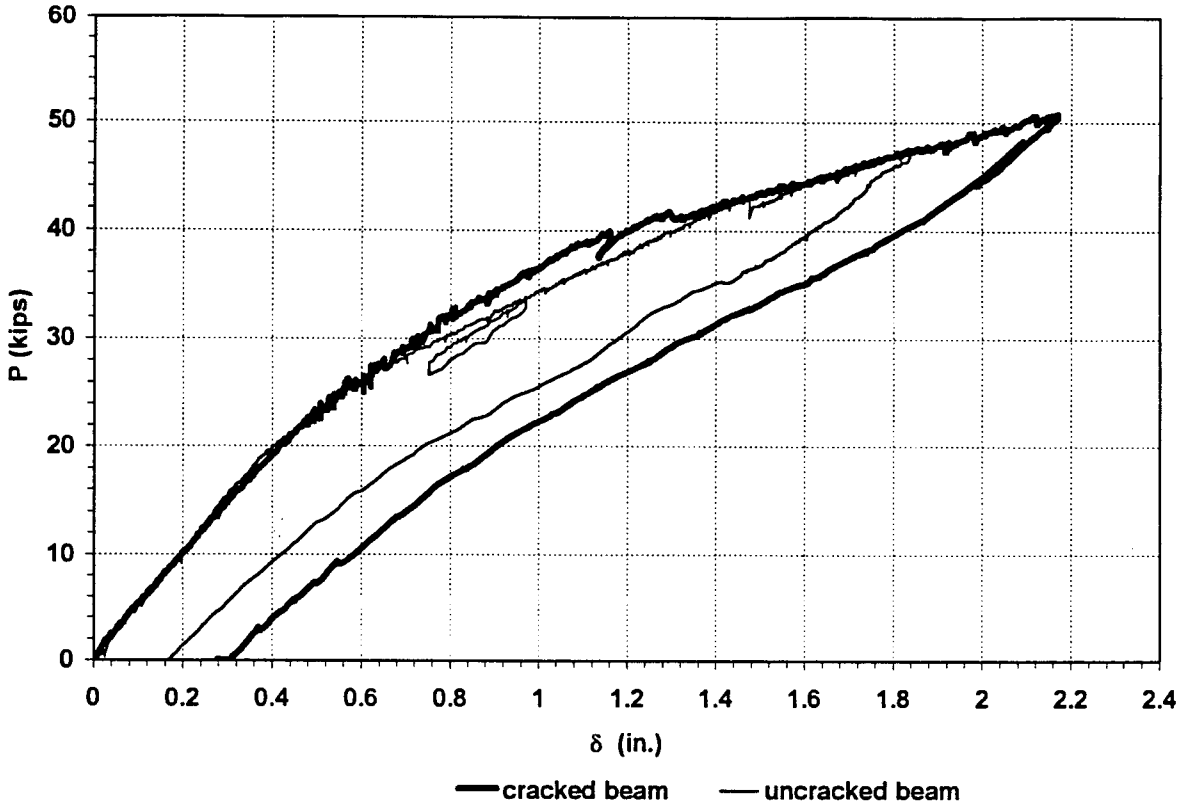


**Figure 3.13 - Load vs. deflection - east load point - cracked and uncracked beam responses.**

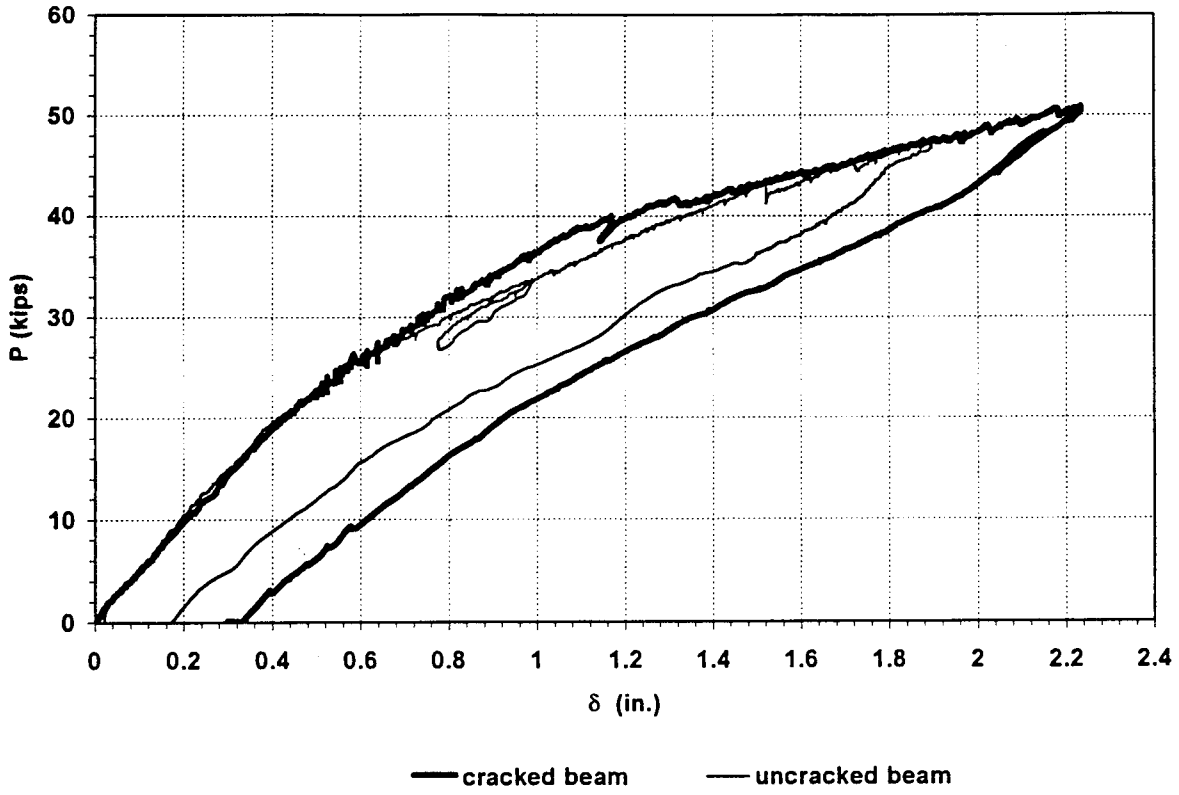


**Figure 3.14 - Load vs. deflection - midspan - cracked and uncracked beam responses.**

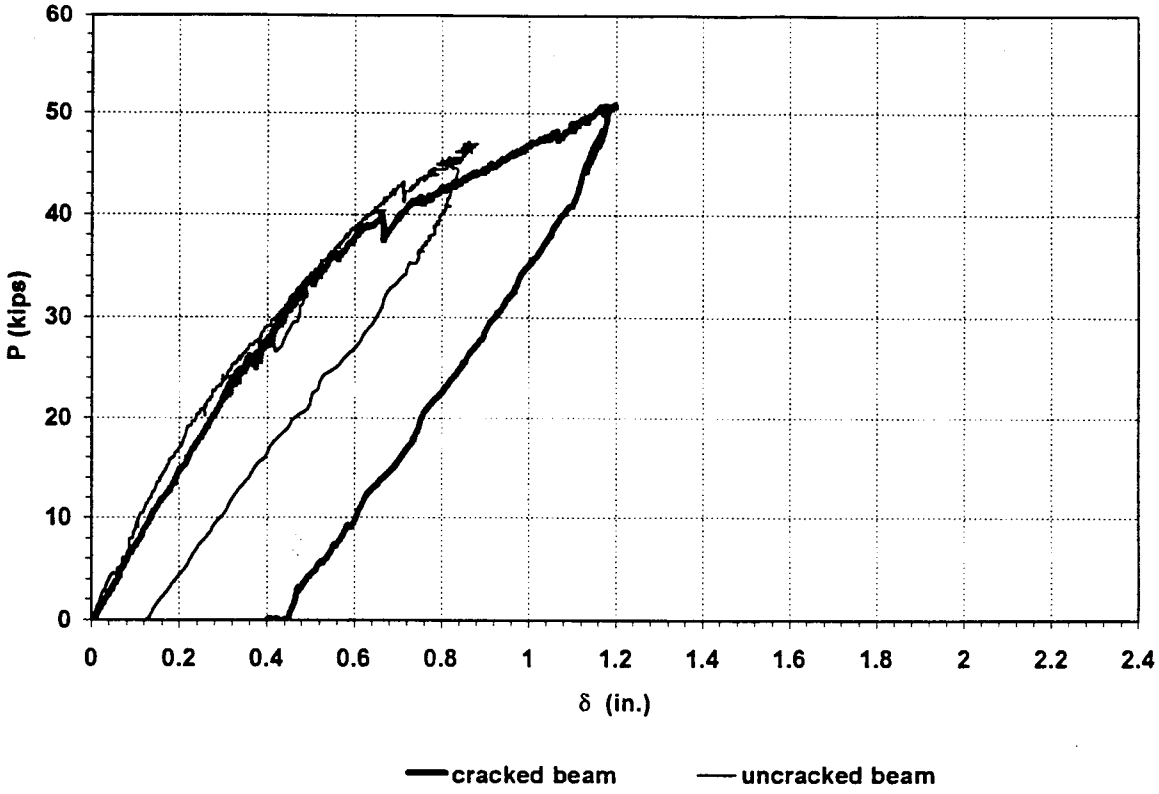


**Figure 3.15 - Load vs. deflection - west load point - cracked and uncracked beam responses.**

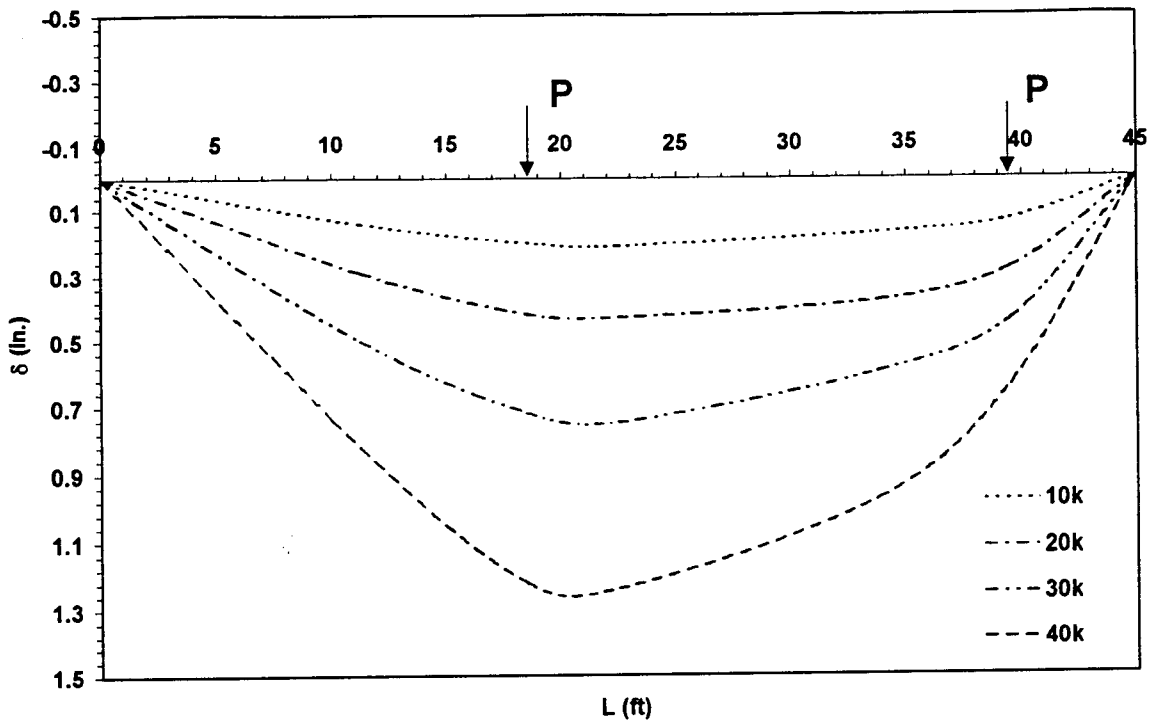


**Figure 3.16 - Deflection profiles - cracked beam - load positions shown.**

THIS PAGE INTENTIONALLY LEFT BLANK

# CHAPTER 4

# CONSTRUCTION AND TESTING OF THE REPLACEMENT STRUCTURE

## 4.1 Fabrication of the New Beams and Construction of the New Bridge

The new beams for the replacement structure were fabricated at Prestress Services, Melbourne, Kentucky. Since this site is near the University of Cincinnati campus, members of the UC research team were present during fabrication.

At the time the new beams were fabricated, the old beams had not yet been removed from the bridge and cause of failure in the old beams was not yet known. However, it was suspected that the problems were related to the termination of the mild steel in a tensile zone. As a result, two changes were made:

1) The termination (cut-offs) of the mild steel were staggered, matching the skew, rather than being all the same distance from the obtuse corner.

2) Extra stirrups were added in this area to double the area of shear steel available.

Except for these changes, the beams were fabricated according to applicable ODOT standards. At the time of fabrication, the UC research team installed vibrating wire strain gages in the #7, #8 and #9 beams.

After removal of the old bridge beams, the tops of the existing abutments (beam seats and back walls) were removed (recall that the beam seats had been poorly finished and were uneven, resulting in uneven bearing of the beams). These items were recast to specification before the new beams were installed. The new beams were installed and the composite deck was cast and cured. When the new bridge was tested one year after construction, no cracks were present.

## 4.2 Testing of the New Bridge

After construction of the new bridge, a static truck load test was done. As before, four, single axle ODOT dump trucks were used in a total of eight load combinations. Figure 4.1 shows the instrumentation plan. It differs from the original instrumentation plan as follows:

1) Instruments which were placed on cracks in the first test were eliminated in the second test as there were no cracks in the beams.

2) Instead of using external clip gages to measure strain, internal vibrating wire strain gages were installed during fabrication.

3) Deflection measurements were taken under every beam (note: the instrument placed on beam #3 failed during the test so the results are not presented).

4) Deflections were not measured at the supports since the beams had been properly shimmed. Figures 4.2 - 9 show the results of the truck load testing (truck weights are in Table 4.1).

**Case 1 (Figure 4.2):** The trucks are placed with back axles along the centerline of the bridge. This maximizes moment at the midspan. Deflections are not uniform with the beams on the NE side of the bridge (beam #1) deflecting more than those on the SW side (beam 9). These deflection decrease about 20% from beam 1 to beam 9, probably because of the effect of skew. There is a slight uplift on the corners along the southeast edge. It appears the bridge behaves as one way, skewed slab.

**Case 2 (Figure 4.3):** For this case, the trucks are parked with the front axles along the centerline of the bridge. In this configuration, shear is maximized on the northwest edge of the bridge (this is the edge where the diagonal cracks were found in the #9 beam in the original bridge). The deflection of the #9 beam is about half that of the #1 beam. This again seems to be caused by the skew, with the obtuse corner being stiffer than the acute corner.

**Case 3 (Figure 4.4):** This case examines the effect of skew. The first truck is placed with the front axle at midspan of the #8 beam and the other trucks are set so that the front tires are aligned. Although the truck loads do not follow the skew, the deflections are uniform.

**Case 4 (Figure 4.5):** For Load Case 4, four trucks are placed bumper to bumper in the lanes, all facing southeast. This attempts to maximize lane load and shear at the northwest edge. Although the bridge appears uniformly loaded, beams 4-9 appear to carry most of the load as they have the largest deflections. Again, there seems to be a flow of load to the obtuse corner.

**Case 5 (Figure 4.6):** In this case, the trucks are placed in the lanes, but "back-to-back". This maximizes lane load and moment. As with Cases 1 and 4, the apparently uniform loading pattern produces nonuniform deflection.

**Cases 6, 7, 8 (Figure 4.7,8, 9):** These load cases reflect various placements of the trucks meant to maximize the load on beams #7, #8 and #9. As expected, the deflections of beams 5-9 are greater than those of beams 1-4.

It is clear from the test results that effect of skew, and perhaps superelevation, are pronounced. In cases of apparently uniform loading, it is clear that load flows to one side or the other of the bridge. This helps to explain why the beams 7-9 failed in the original bridge. Not only were these beams heavily loaded by full coal trucks, but there was also a tendency for load to flow to this side of the bridge in certain load patterns.

It is clear from the measurements that the loads in the individual beams are not large. This is shown by the extremely small deflections and strains. The largest measured strain was $50 \times 10^{-6}$,

measured in beam 9 in load case 7 (four trucks placed on the SW side of the bridge, Figure 4.8). This corresponds to a live load tensile stress of about 250 psi at the gage position, which is approximately 3" from the bottom of the girder (midheight of the bottom flange). The measured strain can be extrapolated to a maximum bottom fiber tensile stress of about 320 psi. Even if the precompression from the prestressing is taken as 0 (i.e. an extreme case of 100% loss of prestress), the maximum measured stress is still 25% below the allowable tensile stress. Thus, the new structure seems to be very satisfactory.

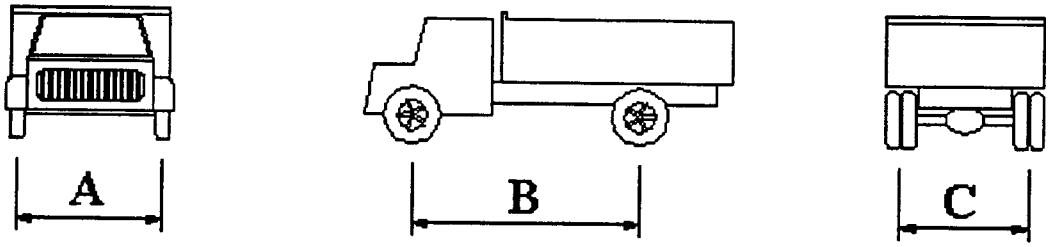


| Number | Front Axle Pounds | Rear Axle Pounds | Total Weight Pounds | A in. | B in. | C in. |
|---|---|---|---|---|---|---|
| 639 | 9300 | 25300 | 34600 | 80 | 137 | 141 |
| 528 | 9240 | 24900 | 34140 | 80 | 137 | 139 |
| 814 | 9800 | 26600 | 36400 | 80 | 137 | 139 |
| 747 | 10080 | 24900 | 34980 | 80 | 137 | 139 |

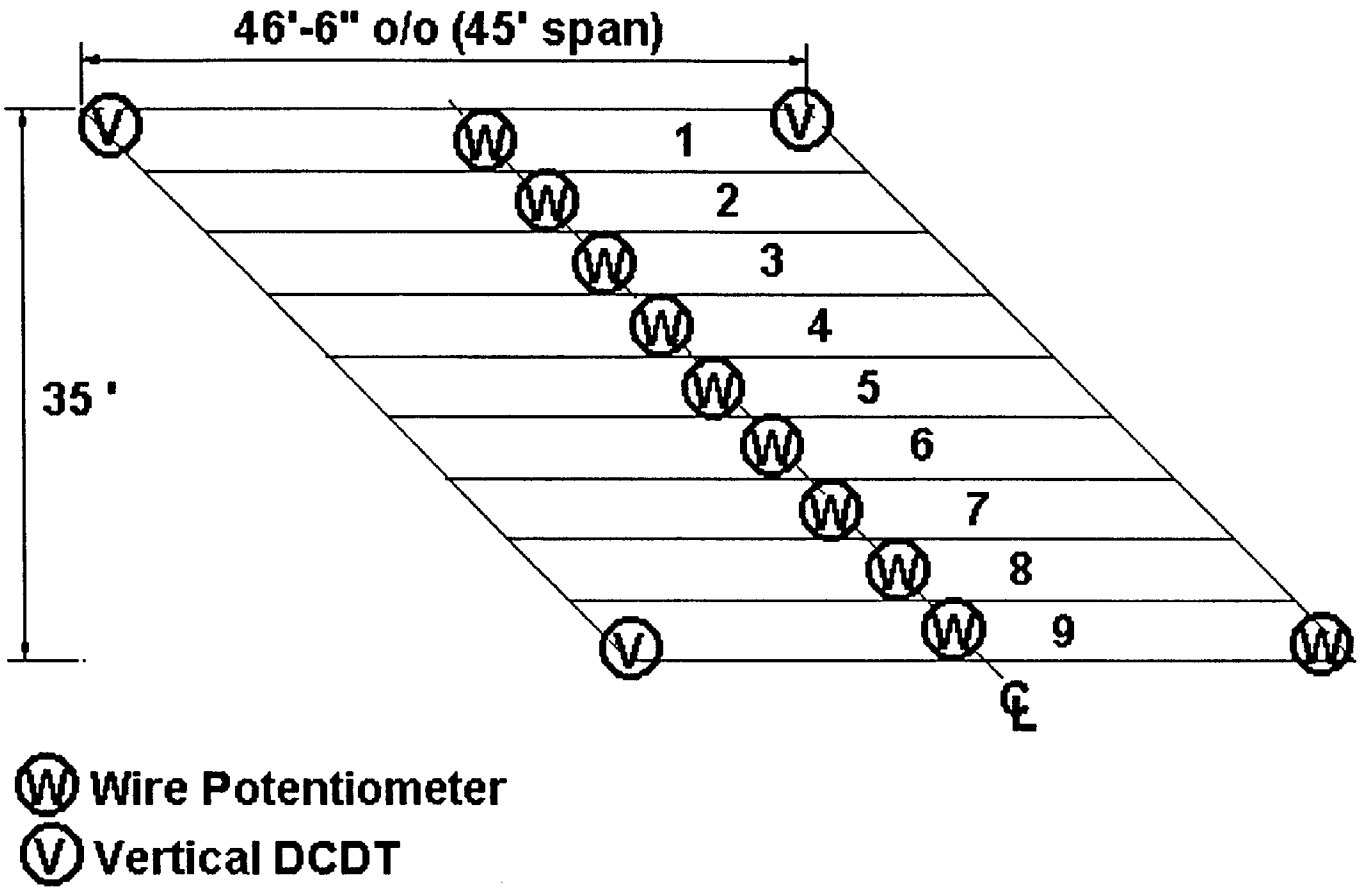


**Figure 4.1 - Instrumentation plan.**

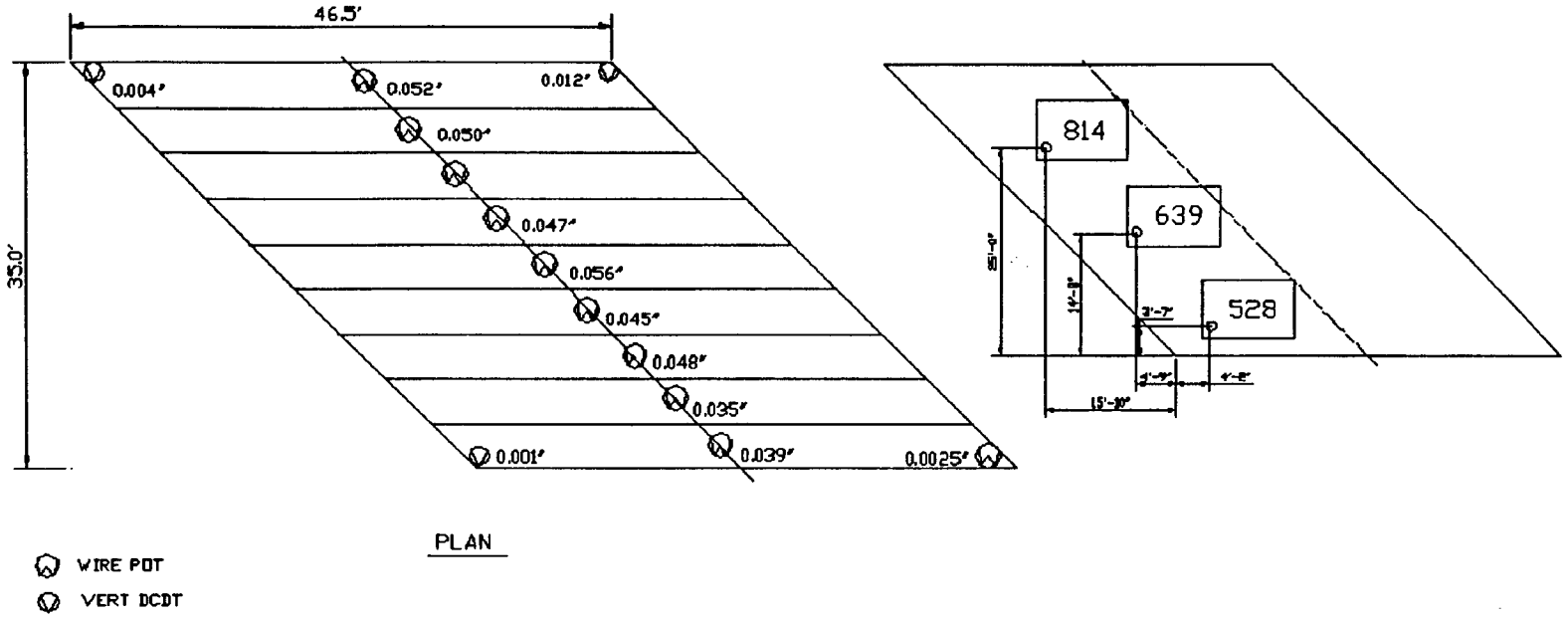


**Figure 4.2 - Load case #1**

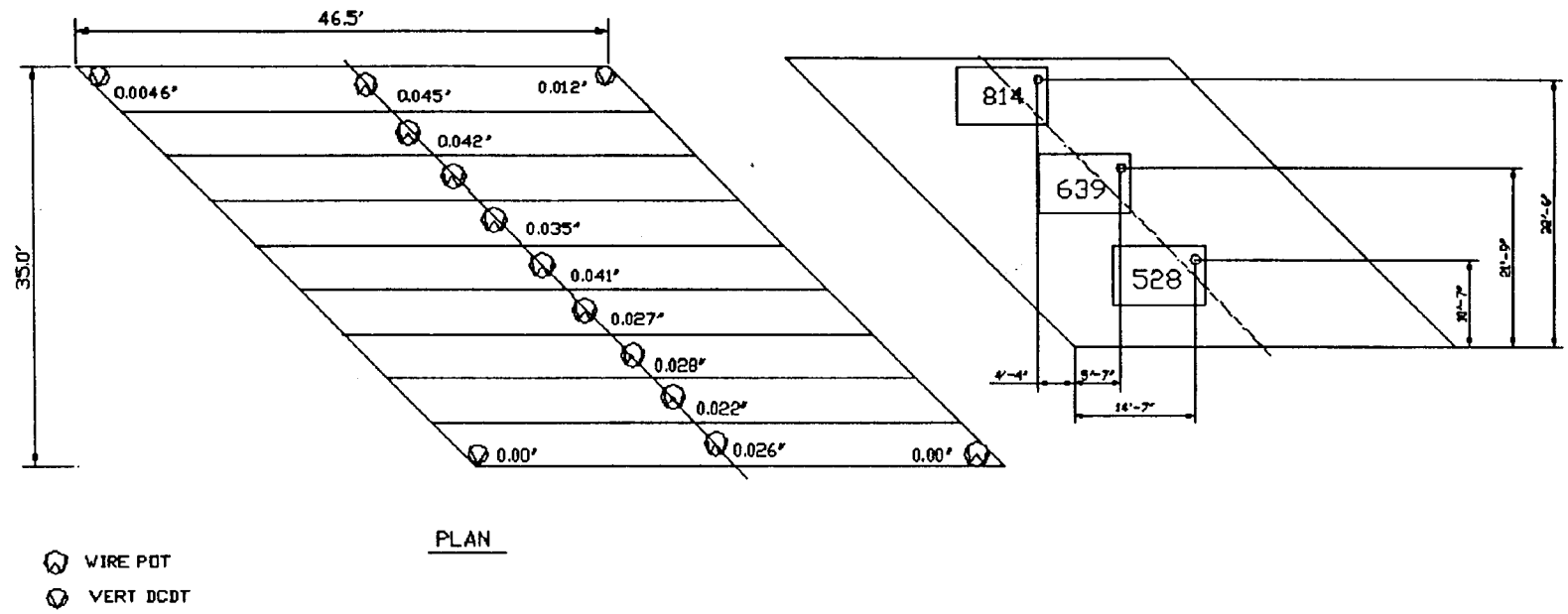


**Figure 4.3 - Load case #2**

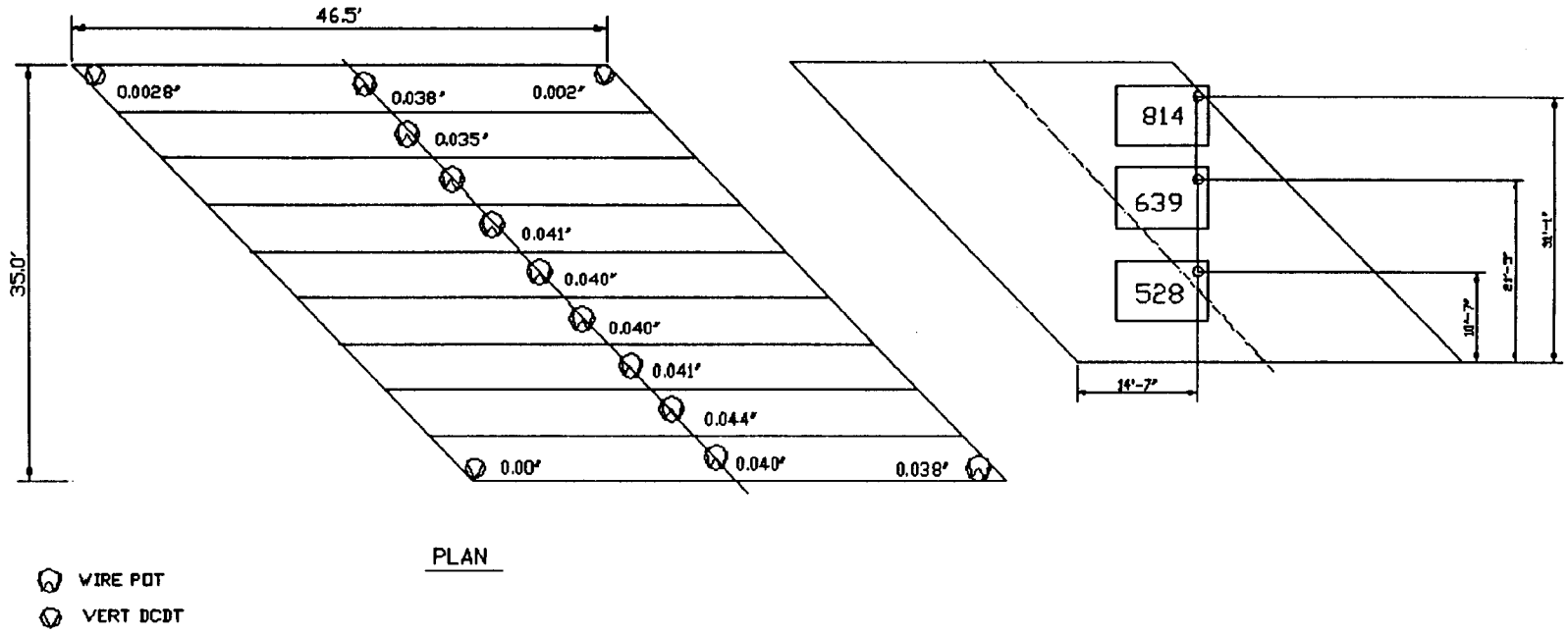


**Figure 4.4 - Load case #3**

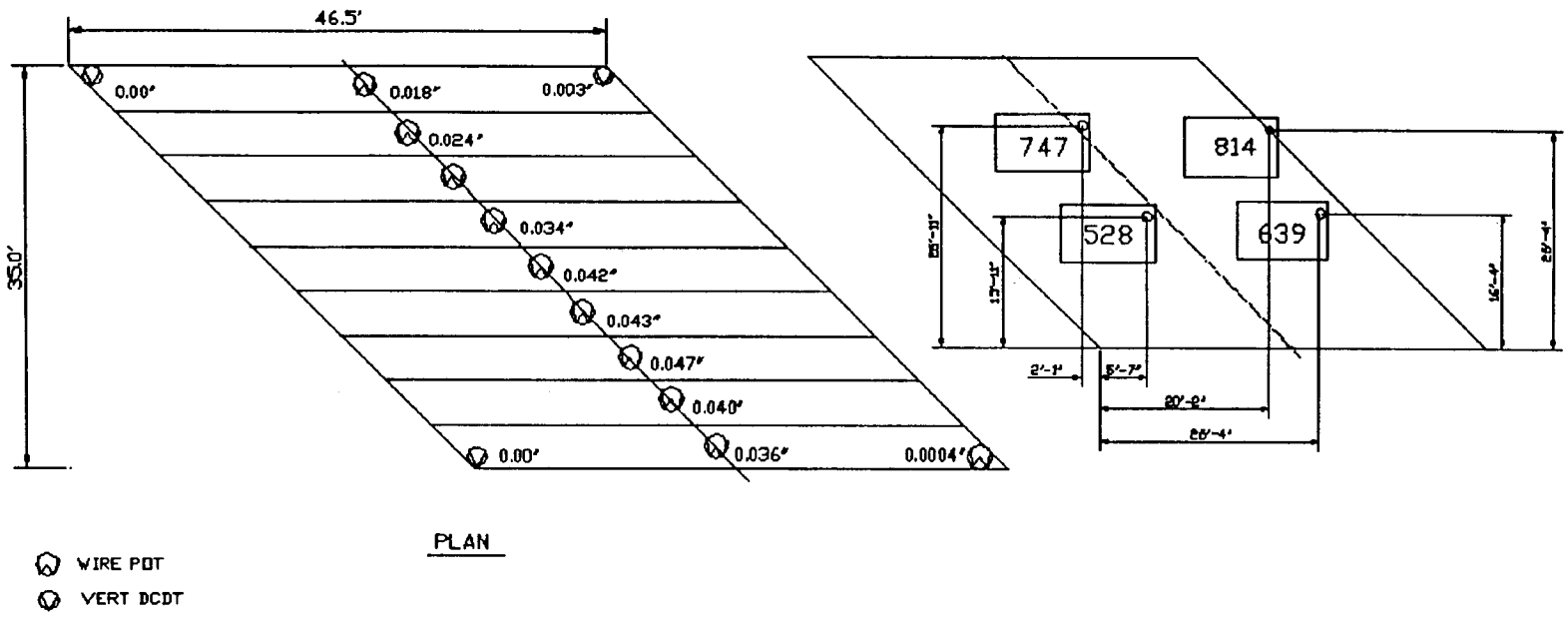


**Figure 4.5 - Load case #4**

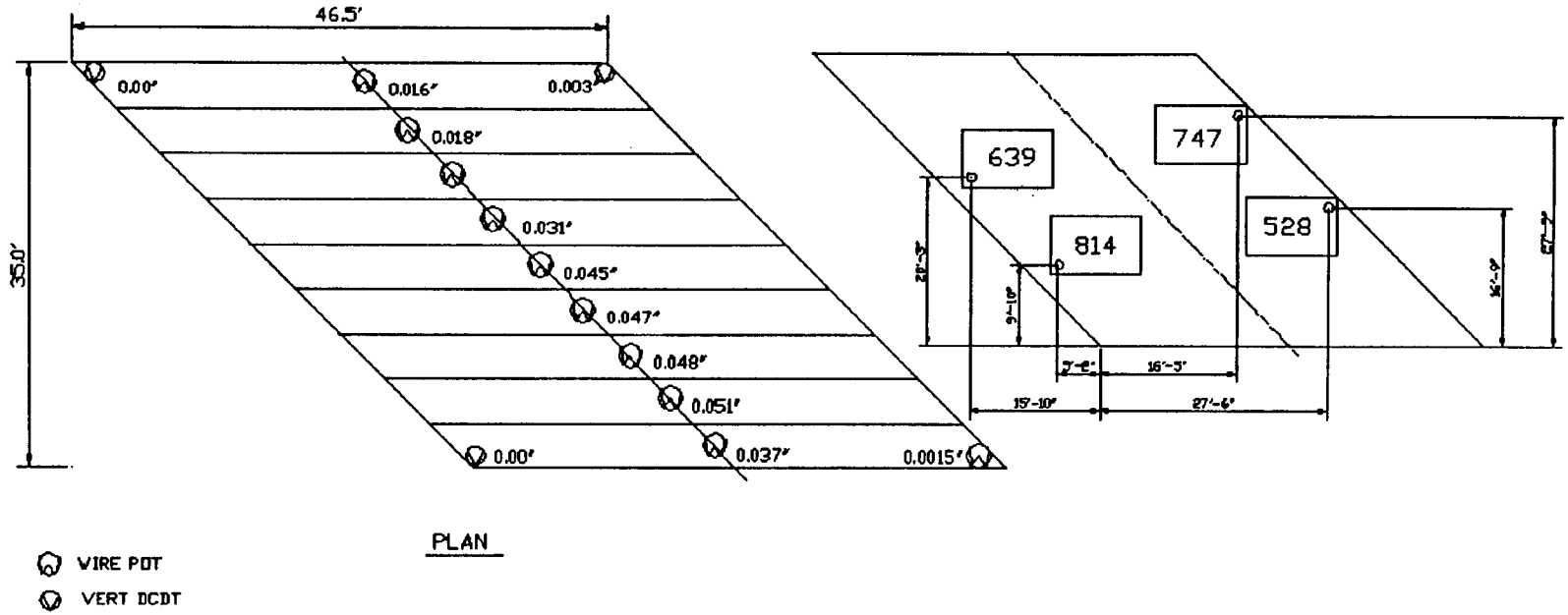


**Figure 4.6 - Load case #5**

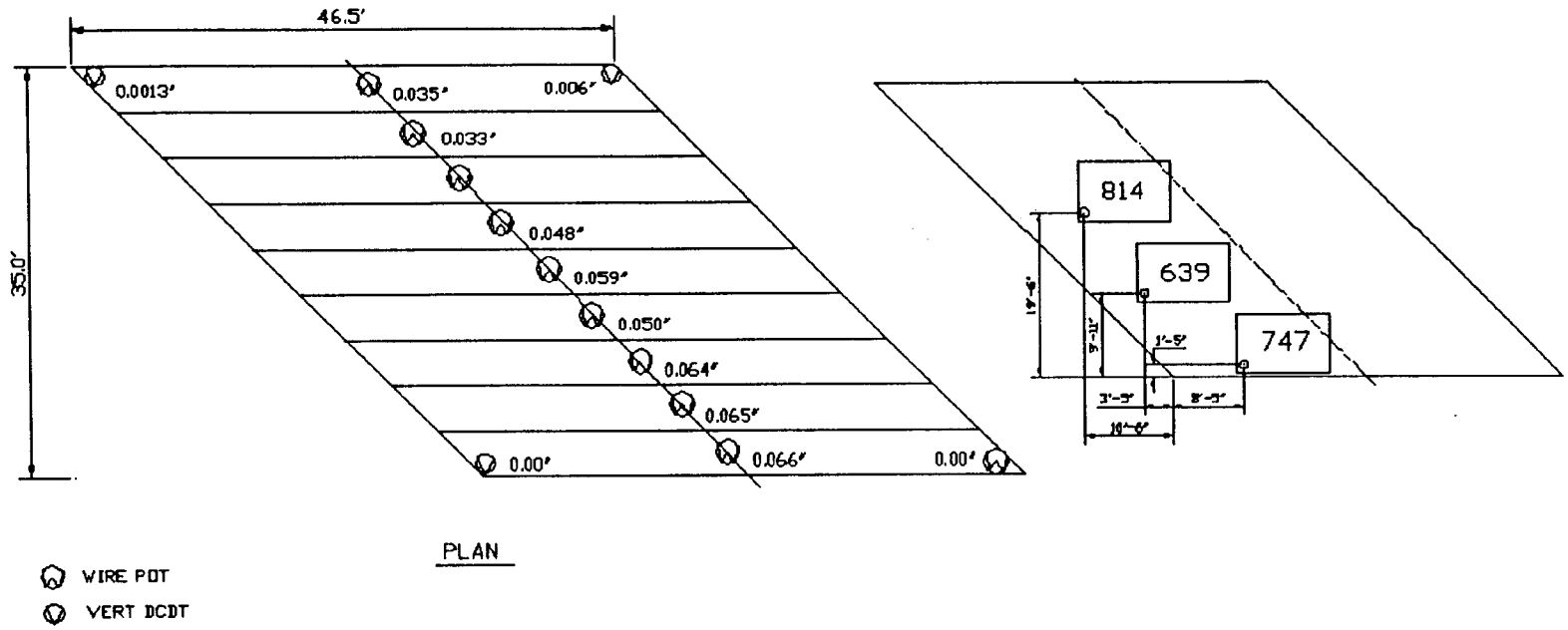


**Figure 4.7 - Load case #6**

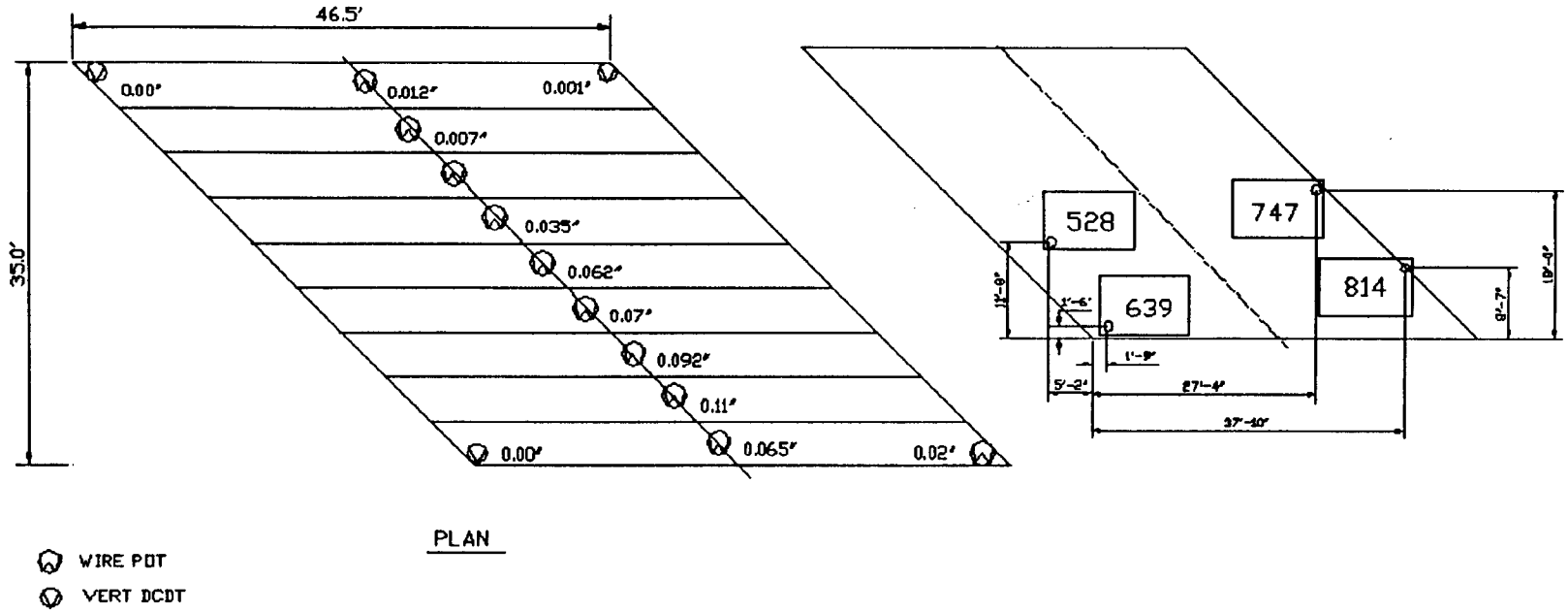


CASE #7

**Figure 4.8 - Load case #7**

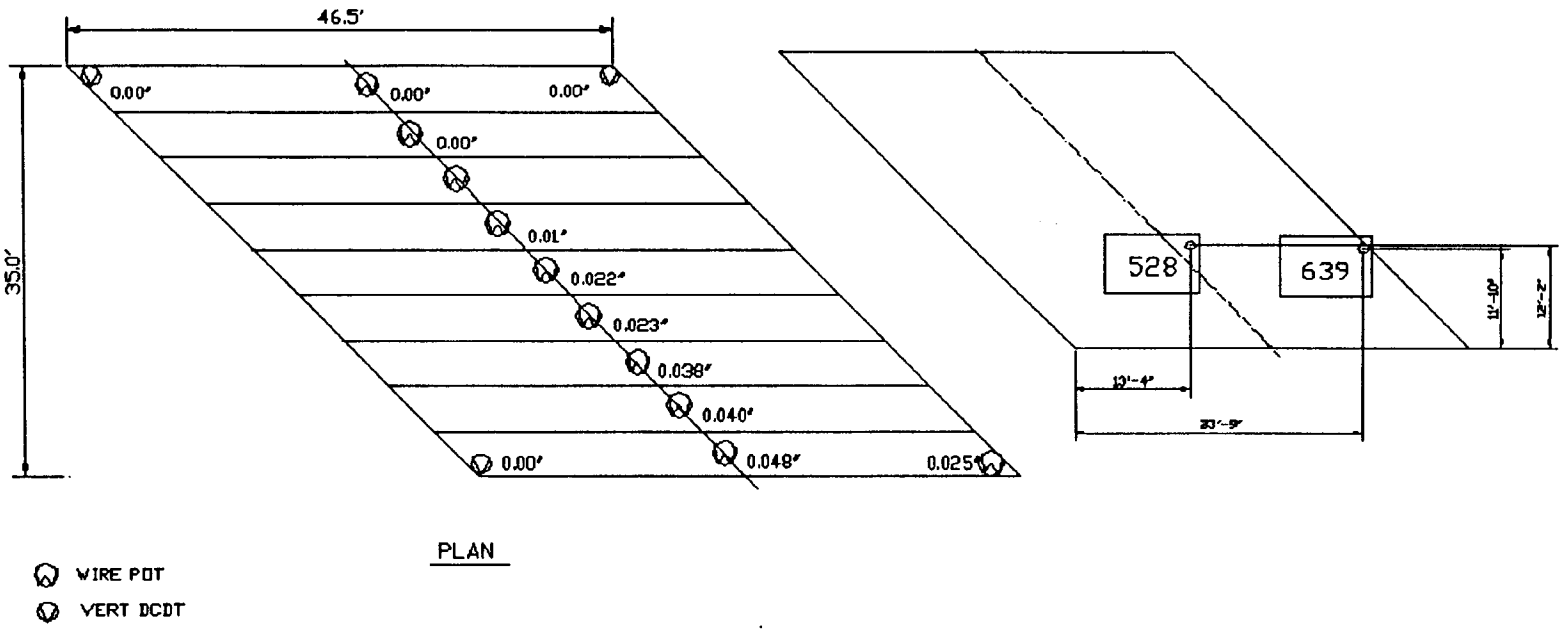


**Figure 4.9 - Load case #8**

THIS PAGE INTENTIONALLY LEFT BLANK

# CHAPTER 5

# FINITE ELEMENT ANALYSIS OF THE BEAM

## 5.1 Introduction

Experimental evidence presented in Chapters 3 and 4 showed that the bridge failed due to an error in debonding the strands. However, there is a question at whether this alone was the cause of the failure or if other factors , such as detailing of the mild steel or the skew, may have contributed to the failure. In order to assess the impact of these other factors, a single prestressed box beam was modeled by the finite element method. The model was created to match the destructive test (performed on a single beam), therefore the bridge deck slab was included in the numerical model but the analysis did not consider effects of adjacent members. There were three primary reasons for performing the finite element analyses:

1) To ascertain whether the cracking which had been observed in the real beam was caused by factors other than fabricator error and if the cracking could have been anticipated if detailed numerical analysis had been completed prior to the fabrication and erection of the beams.

2) To investigate the distribution of stresses throughout the beam in more detail than possible using experimental testing alone; and

3) To observe the variations in response (including stresses, cracking and deflections) which could be anticipated if the box beams had been constructed using details other than those employed in the real beams.

Several finite element models were created: one corresponding to the details of the beams used in the real bridge, and other models representing modifications to the arrangement of reinforcing steel and debonding patterns for the prestressing tendons. The load case from the destructive test (two point loads placed as shown in Figure 3.5) was used in all finite element analyses.

When using the finite element method, the analyst must make strong efforts to verify the reasonableness of the model and to compare, whenever possible, the numerical results to known solutions or experimental results. When modeling a simple system composed of a Hookean material with relatively small displacements, it is generally expected that the finite element analysis gives very accurate results. However, the present circumstance involves some more complex issues: modeling concrete (which is non-Hookean at high compression stress levels and also cracks under low tensile stress); approximating the behavior of a concrete and steel composite; representing a prestressed condition; and investigating nonlinear response to applied load. Therefore, comparison of numerical results to experimental results is an essential step in establishing confidence in the numerical results of the finite element analysis. If the finite element model which represents the actual beam as closely as possible gives results which reasonably match the experimental results, then and only then the model may be expected to accurately predict the effects of modifying the details of the reinforcement.

Consequently, the finite element results presented here supplement the experimental results and simultaneously rely upon the experimental results for verification of accuracy.

## 5.2 Analysis Prior to Testing

Prior to conducting the destructive load tests, some simple analyses were performed. A computer program called "RESPONSE", which models the prestressed beam as a series of lengthwise segments and considers the moment-curvature relationship of each segment, was employed to predict general response, identify points at which flexural cracking might develop, and characterize the load-displacement relationships for critical points along the length of the beam. Results from this preliminary analysis were used to guide the experimental program, to suggest approximate load magnitudes that might cause cracking and to indicate points at which wire potentiometers would be placed to best represent the displacements of the beam under various load levels. The load versus deflection results from RESPONSE were not expected to have great accuracy since this program does not model all features of the prestressed concrete beam characteristics, however, it did provide a very reasonable approximation of the beam behavior (see Figure 3.9-3.11).

## 5.3 Application of the ANSYS Finite Element Program

Several commercial finite element programs were initially considered for use in this project. After detailed comparison of the features of the programs available at the University of Cincinnati, and in view of expecting to use over 14,000 elements and 18,000 nodes, ANSYS was selected for the investigation since it has a readily accessed element to represent the concrete/steel composite behavior, requires less labor for modeling related input with a manual-graphic input mode, and has an excellent post-processor for output representation.

The following sections briefly describe a few of the most pertinent features of the modeling of the prestressed concrete box beam. Additional details of the ANSYS program may be found in the help file of ANSYS program.

### 5.3.1 Modeling the Reinforced Concrete

In ANSYS, the element called "SOLID 65" can be used for the three-dimensional modeling of solids with or without reinforcing fibers. The element is defined by eight nodes and the isometric material properties, including Young's modulus, Poisson ratio, mass density, and so forth. The element is specified one solid material (concrete in this case) and up to three reinforcing materials. Reinforcing material specifications include material identification numbers, volume ratios and orientation angles. The volume ratio is the rebar volume divided by the total element volume. Reinforced concrete is thus modeled by assuming that the reinforcing steel fibers (rebars) are smeared uniformly throughout the element and act in up to three specific directions as defined by the orientation angles.

The SOLID 65 element is also capable of representing cracking in tension and crushing in compression of the main material. A data table specifies the characteristics of the concrete material: Shear transfer coefficients, tensile cracking stresses and compressive crushing stresses. The shear transfer coefficient ranges from 0.0 to 1.0 with 0.0 representing a complete loss of shear transfer and 1.0 representing no loss of shear transfer. The values of the various parameters used in the present cases are given in table 5.1.

**Table 5.1 Input Summary for Reinforced Concrete**

| Element Name | SOLID 65 |
|---|---|
| Degrees of Freedom | Ux, Uy, Uz |
| Material Properties | E= 4030 ksi, poisson ratio= 0.25,<br>fc= 5000 psi, fr= 550 psi, Density= 145 #/ft$^3$ |
| Shear Transfer Coefficients | For an open crack, 0.5<br>For a closed crack, 1.0 |
| Properties of Rebars<br>(smeared in SOLID 65) | E= 29000 ksi, poisson ratio= 0.25,<br>yield stress= 60 ksi,<br>after yield, assume E'= 2000 ksi (bilinear model) |

### 5.3.2 Modeling the Prestressed Tendons

The "smeared" approach to modeling rebars in concrete cannot be used for the prestressing tendons since prestress cannot be assigned by a volume ratio representing rebars in SOLID 65. Therefore the three-dimensional spar element, LINK 8, is used to model the prestressing tendons. This spar element may carry only axial force, tension or compression. It has three degrees of freedom at each of its two end nodes, so that it may act in general three-space. In addition to the coordinates of the end nodes, the element is defined by its cross sectional area, elastic material properties, yield stress and initial strain (all of which are constant over the length of the element). The initial prestress is set into the box beam by specifying pre-calculated associated initial strains in the spar elements.

**Table 5.2 Input Summary for Tendons**

| Element Name | LINK 8 |
|---|---|
| Degrees of Freedom | Ux, Uy, Uz |
| Cross Section Area | 0.153 in$^2$ |
| Material Properties | E= 28500 ksi, poisson ratio= 0.25,<br>yield stress= 230 ksi,<br>after yield, assume E'= 2000 ksi (bilinear model) |

In general, each tendon is modeled as a continuous series of LINK 8 element, which runs longitudinally down the length of the box beam. The LINK 8 elements are defined by nodes that are geometrically coincident with nodes that define corners of the SOLID 65 elements and , thereby, the

LINK 8 elements follow edges of the solid elements. The "merge" function of the ANSYS program links the nodes of the LINK 8 elements with the corresponding nodes of the SOLID 65 elements.

The "merging" causes the SOLID and LINK elements to deform consistently, as though perfect bond exists between concrete and tendons. However, perfect bond does not exist throughout the beam, so there are two special effects that must be considered in modeling:

1) In the real beam, a portion of the length of a tendon may be debonded at each end of the beam in order to avoid adverse tension stress in the top of the beam section near the end supports. This debonding is modeled by not merging nodes over the debonded length. Alternately, since no stress develops in the debonded length of tendon, this portion of tendon may be left out of the model.

2) Since the prestressed tendon has no anchorage block and is anchored by bond alone, the prestress is not assumed to fully and suddenly exist at the ends of the bonded length of tendon. That is, it is assumed that the prestress develops over some length of bonded tendon, called the transfer length, that resembles the embedment length which must exist to develop yield strength in ordinary reinforcement. The *AASHTO Standard Specifications* suggests that this transfer length can be taken as 50 strand diameters. In the present analyses, over the several elements within the transfer length, the initial strain was stepped from zero up to that strain which represents the total prestress.

### 5.3.3 Modeling the Supports

The "pinned" support conditions, which are assumed to exist for the simply supported box beams, offer somewhat of a challenge for modeling. If a single transverse line of nodes at each end is supported vertically, to expressly represent the classical view of a pinned support, the support reaction is theoretically applied over a very small area of beam surface. This leads to the prediction of highly concentrated stresses at the support points and this leads to a prediction of fictitious cracking, crushing or other distress over a very localized area. If multiple transverse lines of nodes, or any array of nodes with more than one node along any longitudinal line, are supported at an end, a fictitious end moment reaction is will develop at the support. This, too, will lead to artificially magnified stresses near the beam end.

The solution to this difficulty is to model the support as a thin block of soft Hookean material which spreads the vertical reaction over a small but computationally significant area, thus avoiding stress concentrations. This also permits nearly free rotation of the beam about a transverse axis and thus avoids fictitious end moments of any significant magnitude. This method of representing the vertical support does permit a measurable fictitious vertical free-body displacement of the box beam (due to the average compression of the block of material), but this effect can be estimated and deducted from the vertical displacements of the beam when displacement analysis is a goal of the analysis. The other advantage to this method of modeling the supports is that it closely represents the actual support condition of the beam sitting on an elastic bearing pad.

The SOLID 65 element is used in this analysis to model the support pads described above. The material constituting this pad is assumed to be linear, without possibility of yield, cracking or any other form of nonlinear response. The specific values of input parameters, which are used in the present analyses for the support pad material, are given in Table 5.3

**Table 5.3 Input Summary for the Support**

| Element Name | SOLID 65 |
|---|---|
| Degrees of Freedom | Ux, Uy, Uz |
| Material Properties (linear material) | E= 8 ksi, poisson ratio= 0.40 |

## 5.4 Description of F. E. Mesh and Loading

Three analyses were completed for three different reinforcement patterns and cases of tendon debonding. The overall finite element mesh representing the geometry of the concrete was constant for all cases. Figure 5.1 illustrates the mesh in 3-D view and in elevation view and also shows the support pads. Figure 5.2 shows a cross section of the mesh at a typical hollow section. Diaphragms, as shown in the design drawings, were modeled as solid sections.

The model has over 14,000 elements and over 18,000 nodes. The exact number of elements varies slightly with the particular reinforcing pattern being investigated. The mesh was specified to have neither initial sag nor initial camber prior to prestress definition.

The loading is in the same pattern for all cases, a dead load that consists only of beam weight and two concentrated loads applied to simulate wheel loads. Figure 5.1 shows the position of the applied loads in the model; matching the position of the applied loads from the destructive test (Figure 3.5). These concentrated live loads were applied over rectangular regions at the top of the beam, each loaded region being about 16 inches (longitudinally) by 15 inches (transversely) and were applied along the transverse centerline of the beam. The analyses were completed by starting with full dead load and prestress but zero magnitude live load and then increasing live load incrementally until significant distress was observed in the concrete of the box beam.

## 5.5. Definition of the Three Cases Analyzed

Three different models were analyzed using the finite element method, representing three configurations based on where reinforcing steel (rebars) terminates and where prestressed tendons are debonded. The three cases are illustrated in Figures 5.3-5.5. In Case 1, the rebars all terminate along a line which is perpendicular to the axis of the beam and all the tendons are debonded to the point where the rebars terminate. This represents the "as built" condition for the original structure. In Case 2, all the rebars are the same length and therefore terminate along a line which is parallel with the skewed end of the beam, but the tendons all terminate along a line perpendicular to the longitudinal axis of the beam at the obtuse corner. This represents the "as built" condition for the

replacement structure. In Case 3, all rebars terminate along a line perpendicular to the axis of the beam, all tendons continue past this line, towards the beam end, and the tendons do not all terminate along a single line, half are debonded to the obtuse corner and half are debonded to the termination of the steel. The represents a middle position between the "as built" condition for the original bridge (where the tendons are debonded to the termination of the mild steel) and the original design (where the tendons are debonded to the obtuse corner).

Each model includes 4 kinds of material (concrete, reinforcing steel, prestressed steel tendons, and elastic support pad material) and 2 element types (Solid 65 and Link 8). In order to define material properties and the distribution of reinforcement in the Solid 65 elements with "smeared" reinforcement, it is necessary to define 29 constants numerically in each case. The values used for Young's moduli, yield stress, and so forth for each material have been specified in preceding sections of this report.

### 5.5.1 Case 1

Case 1 is intended to represent the actual rebar placement and tendon debonding, as believed to exist in the beams which were tested. In this model all rebars are terminated at the debond points that lie along a line perpendicular to the longitudinal axis of the beam and are 80" away from the extreme end point. Details of the reinforcement and tendon layout are shown in Fig 5.3.

The finite element analysis showed that the maximum longitudinal stresses did not occur at midspan. Stresses at the West end of the beam were the largest, as expected, because one of the concentrated loads is applied near that end. However, large stresses are also seen at the East end as well. These maximum longitudinal stresses occupy a region which slopes upward from the bottom of the beam towards mid-depth. For a given end of the beam, the stresses are not symmetrical from side to side with the higher stresses being found near the obtuse corner.

The cracking load was about 12 kips/point. This is much lower than the actual value of 23 kips/point found in the test. The cracking load is a function of the material properties. Design strengths rather than actual strengths were used for the concrete and there are also other parameters which are unknown and cannot be found accurately (e.g. condition of friction across the crack). Usually, an initial FEM analysis is made using assumed properties and the properties are the adjusted (or *tuned*) to make the model fit. However, in this case the purpose was to compare different designs and tuning would affect all the designs the same. Since a comparison of the different designs was desired (and since a single load step took 18-24 hours to run), it was decided to use the untuned model results for comparison. The crack patterns would be unaffected by tuning.

Figures 5.6 and 5.7 show the predicted cracking in the beam at a load of 40 kips at each load point. The model shows no flexural cracking at the midspan and diagonal cracks formed at each end of the beam. The diagonal cracks are consistent with the test beam, although the test beam did show a very small amount of flexural cracking at the midspan which the model did not predict. However, the overall cracking of the beam is very well predicted by the model.

### 5.5.2 Case 2

The model for the beam in Case 2 is the "as built" condition for the replacement structure. In this model, the tendons are properly debonded to the obtuse corner. Iin the replacement structure, the mild steel cut-offs were staggered and this was duplicated in the model (Figure 5.4). This case was modeled to determine if the replacement structure was likely to crack.

For Case 2, the maximum stresses occurred at midspan, not near the supports. The crack patterns, shown in Figure 5.8, indicate that normal, flexural cracking would occur. This cracking was predicted to occur at a load between 35-38 kips/point; significantly higher than the 23 k/point found in the real test. Therefore, the output from Case 2 suggests that if the beams for the replacement structure were tested, the cracking pattern would be significantly different than that observed in the original structure. This analysis also indicates that the replacement structure will safely carry imposed loads without cracking.

### 5.5.3 Case 3

This case is a compromise between the conditions of Case 1 and those of Case 2. In this "middle case", 8 tendons are debonded at the same debond points as Case 1 and the other 6 tendons are debonded at the same debond points as Case 2. It was also decided that the rebars would be terminated at the same section (as done in the original design), 108" away from the extreme end point.

For this model, cracking initiated when the load reached 30 kips. The longitudinal stress distributions were very similar to those of Case 2, in which the maximum longitudinal stresses occurred around the midspan. When principal stresses were reviewed, it was found that the maximum principle stress occurred around midspan. This is also the same as case 2. But according to crack graphics (Figure 5.9), it was also found that the crack patterns for this case are not exactly the same as Case 2. Most flexural cracks happened around midspan, but a few flexural cracks were also found at the bottom at one end. Although the results did not show any shear cracks at the end, shear cracks often form from flexural cracks and might appear in the real beams due to complicated loading cycles or dynamic impact which ANSYS could not consider.

Case 3 presents some critical information. Clearly, the results of Case 1 are not unexpected since there is basically an unreinforced section in the beam at the point where cracks occur. Case 2 show that a properly constructed beam will not crack at the supports, but will crack in the middle, as expected. However, Case 3 represents a possible configuration of this beam where the contractor debonds some portion of the strands to limit tension in the top of the beam at the supports. Here, the section is not unreinforced as 50% of the tendons remain bonded to the obtuse corner. The bonded tendons provide more that enough reinforcement to carry the very small moments at the end of this simply supported beam, so no cracking is expected. Yet, the FEM analysis shows cracking. This is probably due to stress concentrations caused by having about 75% of the steel (both mild and

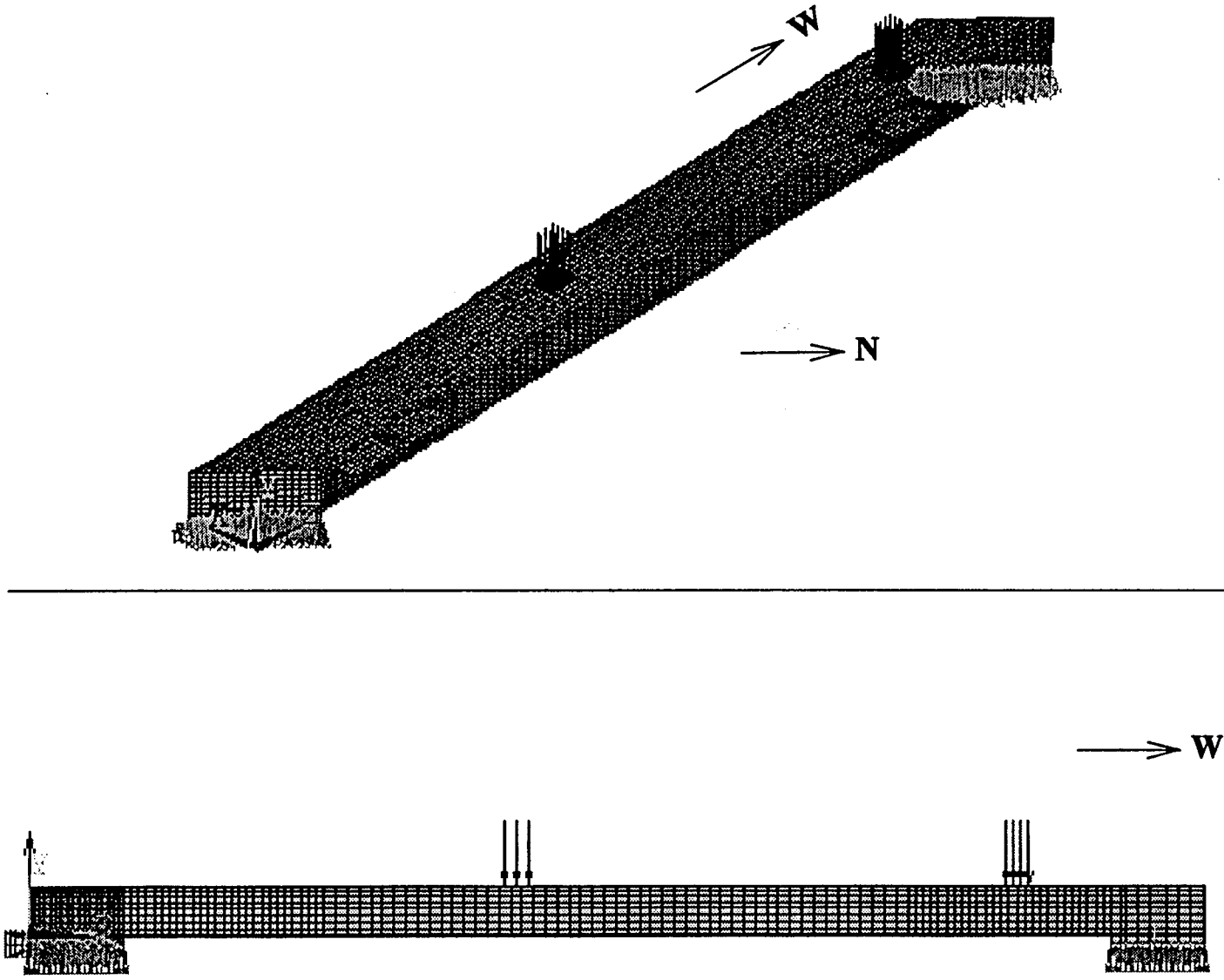


**Figure 5.1 - Mesh and loading**

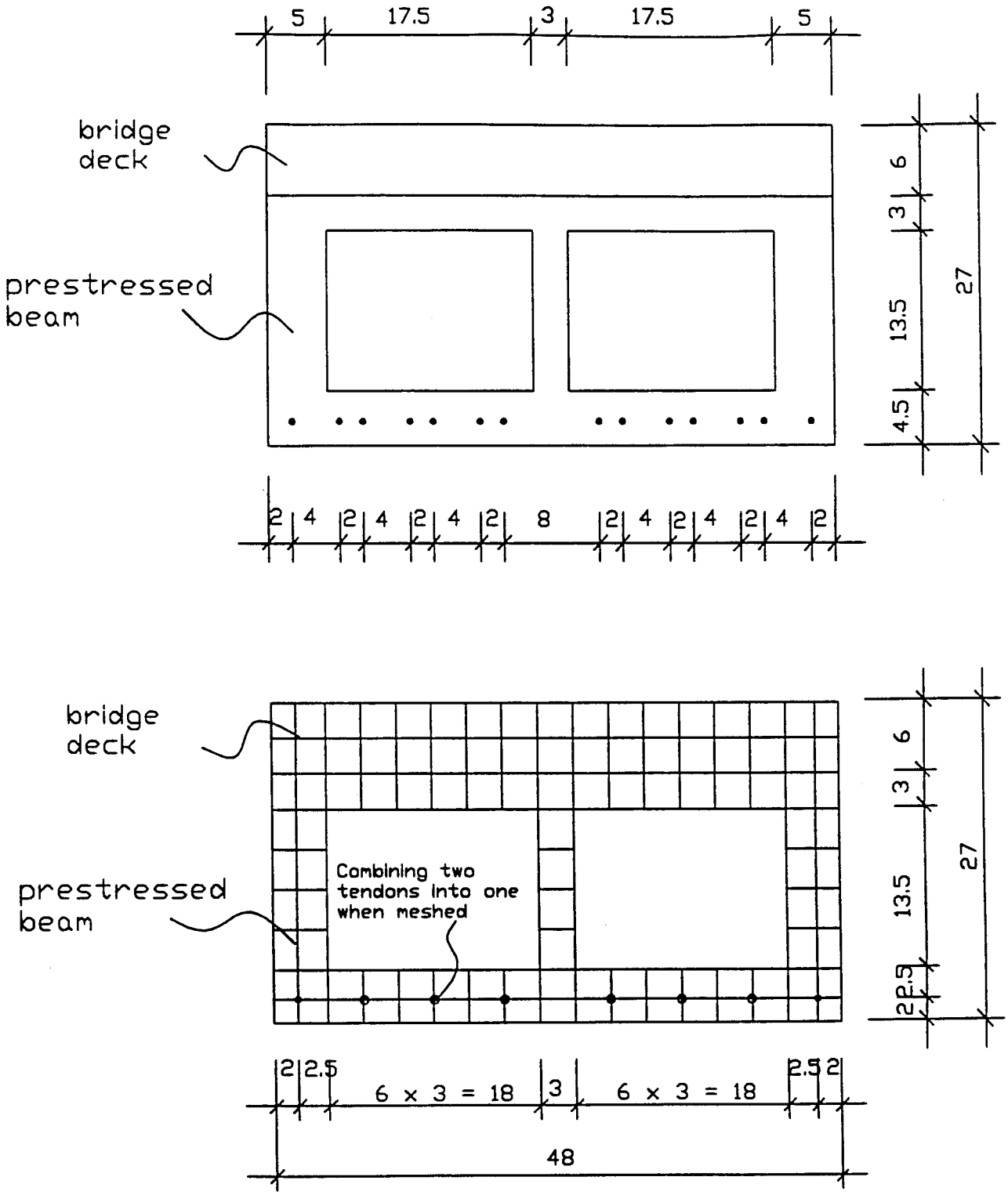


**Figure 5.2 - Mesh cross section**

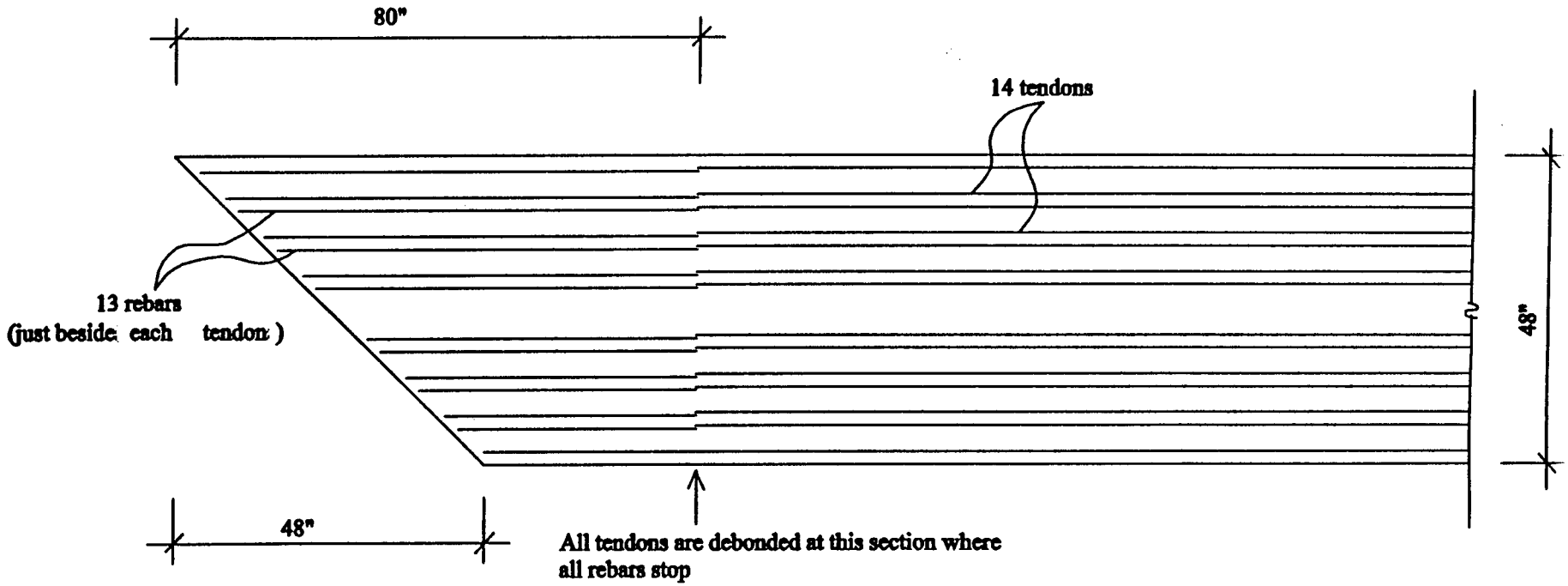


**Figure 5.3 - End condition - Case 1**

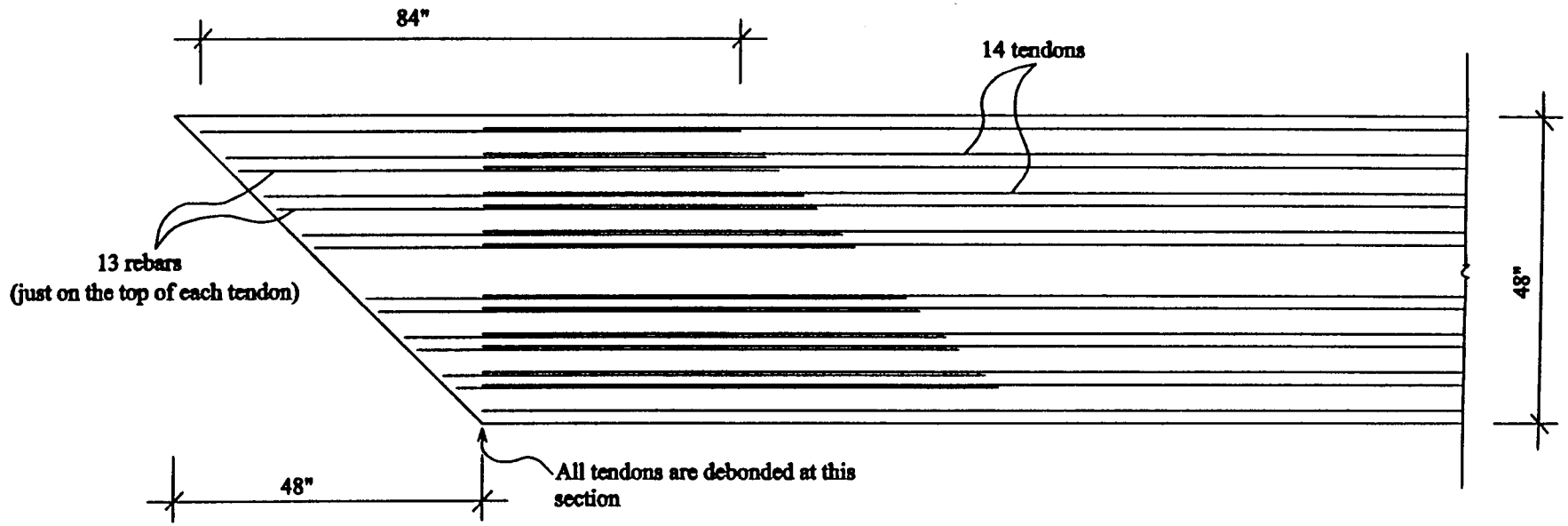


**Figure 5.4 - End condition - Case 2**

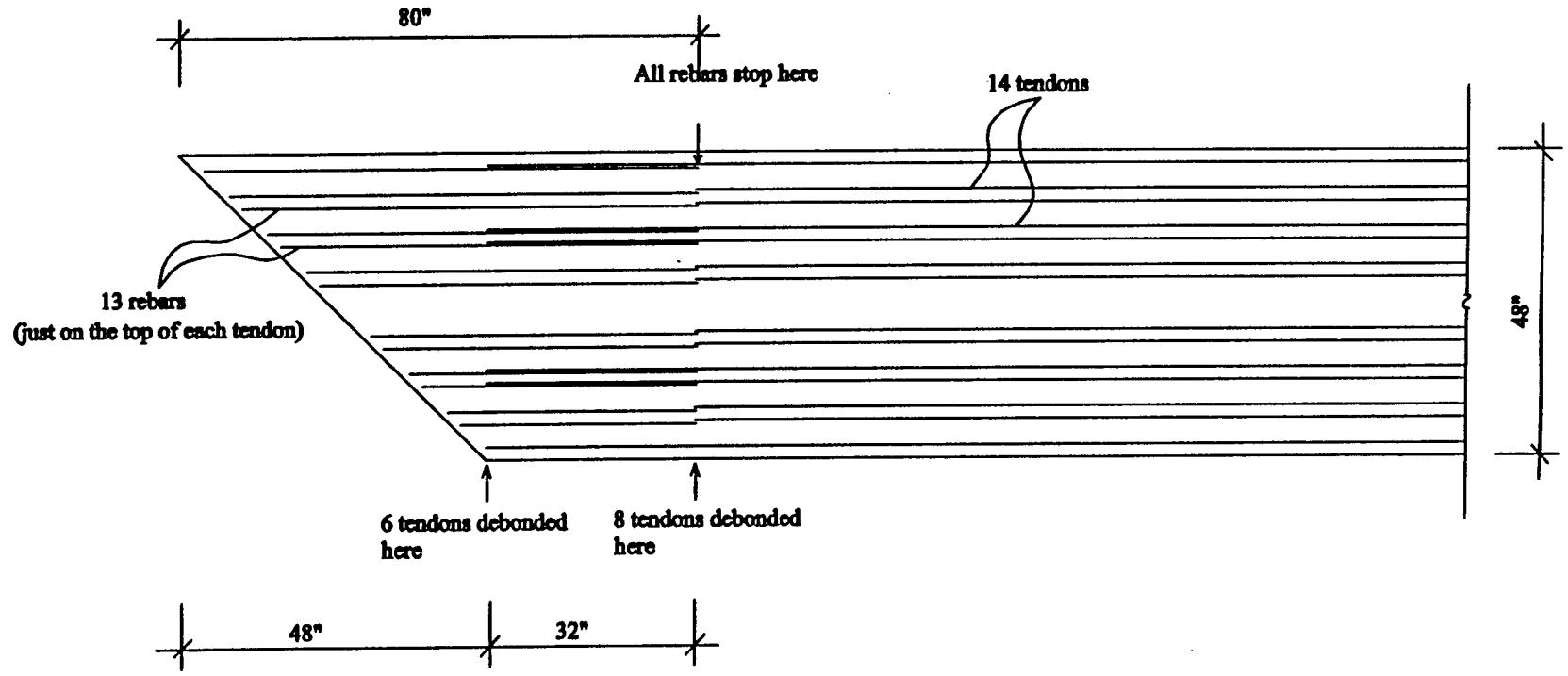


**Figure 5.5 - End condition - Case 3**

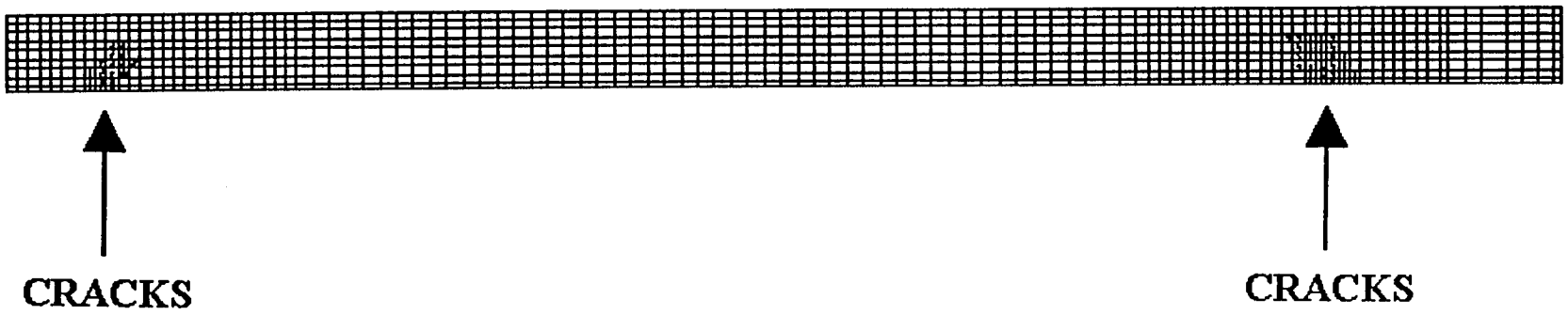


**Figure 5.6 - Crack pattern - Case 1**

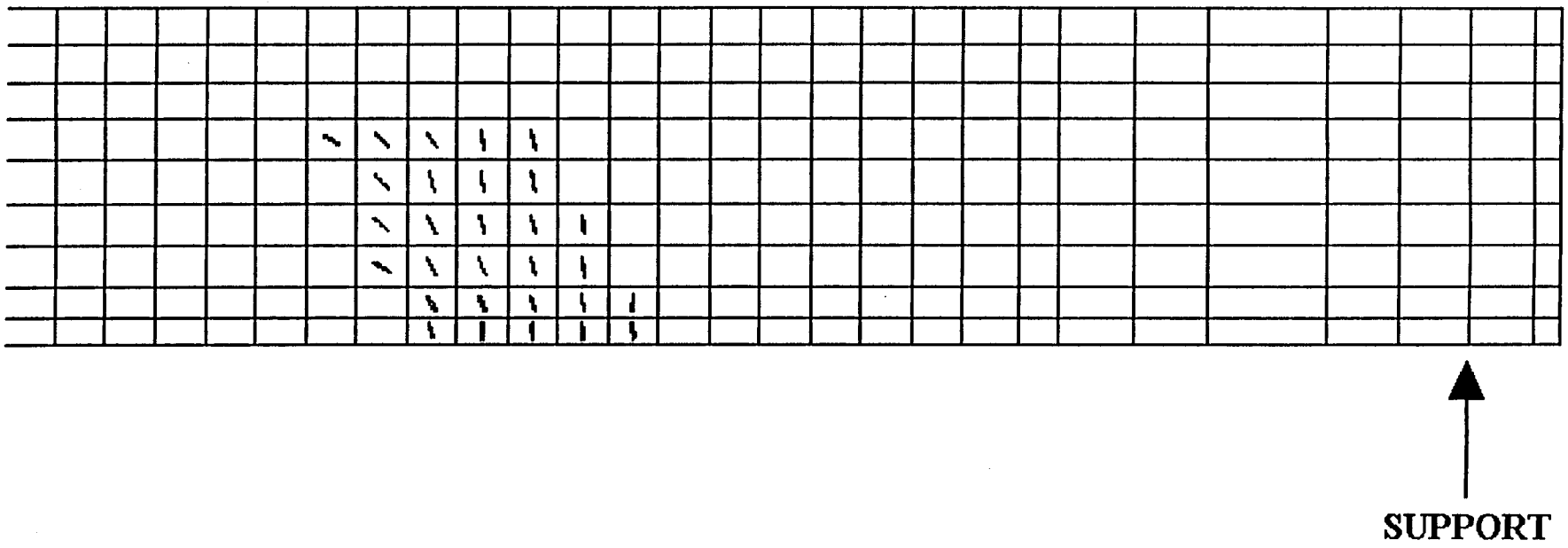


**Figure 5.7 - Enlargement of cracking at end - Case 1**

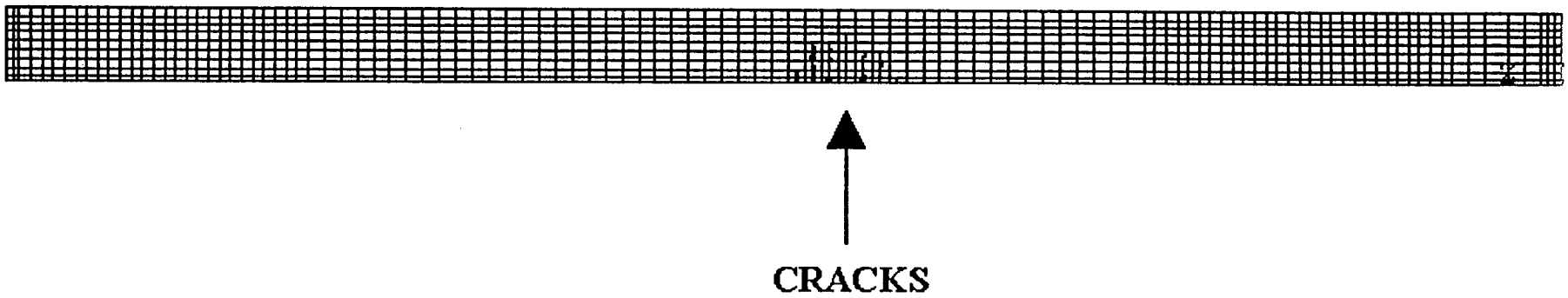


**Figure 5.8 - Crack patterns - Case 2**

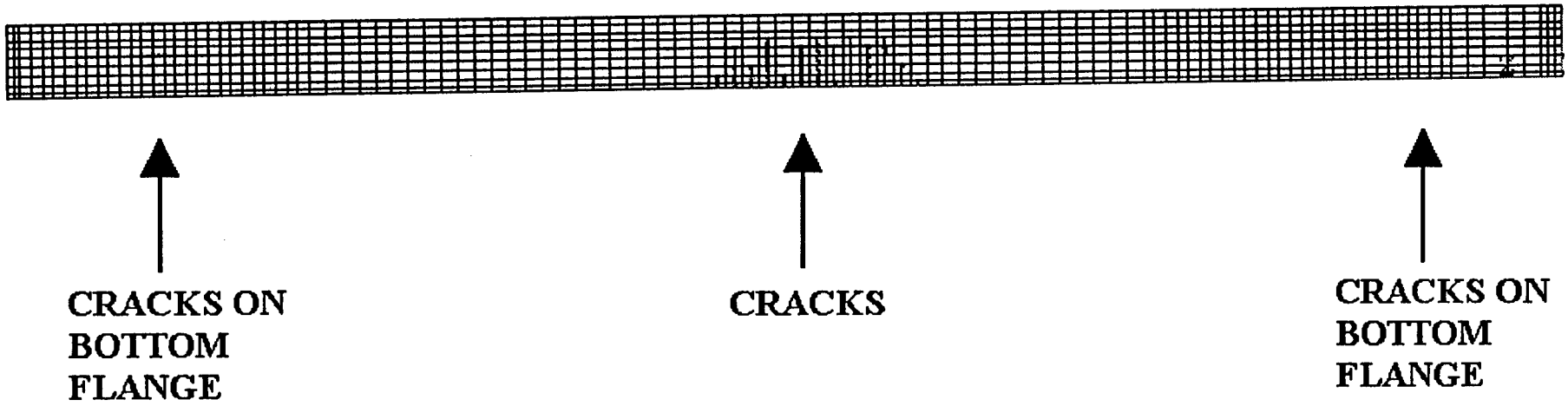


**Figure 5.9 - Crack pattern - Case 3**

# CHAPTER 6

# SUMMARY AND CONCLUSIONS

## 6.1 Summary and Conclusions

Bridge MEG - 124 - 6.78 is located in Meigs County, Ohio on State Route 124 just east of the town of Salem Center. Built in 1994, this structure is a single span, composite, adjacent box girder bridge consisting of nine box girders (eight CB21-48 and one CB21-36) with a 5.5" thick composite deck, a 45'-0" span and a 45° right forward skew. Because it is on a curve, the bridge has a standard superelevation.

One year after construction, cracks were found in the bridge beams. Inspection of the bridge revealed:

1) The beam on the southwest edge had diagonal cracks and straight cracks in the exposed side of the beam, approximately 4 ft. from the obtuse corner. These cracks continued to the bottom of the box where they became transverse (perpendicular to the span). The worst cracking occurred at the northwest corner where the cracks appeared to be diagonal shear cracks. Less severe cracking, which appeared to a vertical flexural crack, occurred at the other end of the beam as well.

2) The two beams adjacent to the edge beam had transverse cracks along the bottom. The sides of the beam were not visible so it could not be ascertained if the diagonal cracks existed along the sides of the beam. Cracking occurred at both ends of the beams approximately 4 ft. from the obtuse corner.

3) The abutments were poorly finished. Due to the superelevation of the structure, the top of the abutments should have had a constant slope. However, the slope was not constant causing the abutment to have a "wavy" appearance.

4) The bearing pads were not tight. It was possible to pull bearing pads out from under some of the beams.

5) The approach slab in the SE corner of the bridge (in the NW bound lane) had a large bump.

A series of static and dynamic truckload tests were conducted on the bridge (see previous report *Investigation of the Cause of Cracking in Bridge #MEG-124-6.78*). It was determined that bridge behaved as single unit so the failure was not caused by overload due to poor load distribution. Torsion was also eliminated as a cause of failure as were excessive dynamic loads.

Since the truck load tests could not determine the cause of failure, beam specimens were removed from the bridge for destructive testing. Two specimens were tested: one which had no cracking and one which was already cracked.

The uncracked beam was tested first. Loading consisted of two point loads, one applied at 7 ft. from the support and one applied at 28 ft. from that same support. The destructive testing showed that the diagonal cracks occurred as soon as the first flexural cracks began to appear, about 23 kips/load point. As load increased, the diagonal cracks grew larger, but the beams held over 50 kips / load point (100 kips, total). When the test was complete, concrete was removed from the bottom and end of the beam.

It was found that the cause of failure was construction error. These skewed boxes were detailed to have all the strand debonded from the end of the beam to the obtuse corner. The area around the debonded strand has conventional reinforcing. This creates a straight beam with a reinforced concrete triangle on the end. In the design, the debonding is to end at the obtuse corner and the mild reinforcing continues past the obtuse corner to provide development length. Unfortunately, the contractor debonded the strands past the obtuse corner to end of the mild steel, essentially creating an unreinforced section. This section failed under load, causing the diagonal cracks. The only reason the section did not collapse is that there is some mild longitudinal steel at this section from assembling the stirrup cages.

The cracked beam was tested next. It was found to have the same behavior as the uncracked beam.

The bridge was rebuilt and the new girders properly constructed. Two changes were made in the new girders. Unlike the original design, which terminated all of the mild steel at the same point, the mild steel termination points in the new girders were staggered. Also, additional stirrups were placed in the termination zone. After the new bridge was constructed, it was tested. The bridge was found to behave as a single unit and there was reasonable distribution of loads between the beams. It was found that the flexural stresses in the girder were very low. No diagonal cracking was observed. The testing confirmed that, properly constructed, the bridge was adequate.

Finally, finite element models of the bridge were constructed. The first model duplicated the "as built" condition of the original bridge; the prestressing strands were debonded to the termination point of the mild steel. The applied loads matched the loading in the destructive test. This model confirmed the crack patterns shown in the actual test - diagonal cracking at the end of the girders. A second model was of the "as built" for the new bridge structure; strand debonded to the obtuse corner and mild steel termination point staggered. The model confirmed that, properly constructed, the girders will not have diagonal cracking at the end and that, under high loads, the beam will exhibit normal flexural cracking at the center of the girder.

The last model was a combination of the first two. In this model, half the prestressing strands were debonded to the termination point of the mild steel. This model showed normal flexural cracking at the midspan, but also showed flexural cracking at the ends. The flexural cracks can grow into diagonal cracks. Because moments at the end of simple span are low, the flexural cracks are not caused purely by moment, but by stress concentrations. The implication is that the stress concentration caused by terminating all the mild steel and some of the prestressing steel at the same point can cause significant cracking. Therefore, the ends need to be carefully detailed to avoid stress concentrations.

It appears that the failure of this bridge was a anomaly, caused by simple construction error. The replacement bridge should perform well, even under heavy traffic.

## 6.2 Suggestions for Future Work

There is no reason why prestressed box girders cannot be used with skews of up to 45°. The detail used by ODOT, which debonds the prestressing strand to the obtuse corner and the conventionally reinforces the ends, will work. But even properly constructed there are problems which need to be addressed.

It is possible that the debonding is not necessary, although there is a concern that the eccentric prestressing force might cause the beams to twist. However, it is not known how much the beams will twist or if adjustments could be made to allow for the twist. If debonding is necessary, studies are needed to avoid details which cause stress concentrations.

## REFERENCES

*AASHTO Standard Specifications for Design of Highway Bridges, 16th Ed.*, American Association of State Highway and Transportation Officials, Washington, DC, 1992.

*AASHTO Guide Specifications for Distribution of Loads for Highway Bridges*, American Association of State Highway and Transportation Officials, Washington, DC, 1994.

Collins, M., Mitchell, D., Felber, A. and Kuchma, D., *RESPONSE*, University of Toronto, 1990.

Miller, R., *Instrumentation of Bridge #MEG 124-6.79*, Report to Sponsors, Ohio Department of Transportation, University of Cincinnati, March, 1999.